NAVAL
POSTGRADUATE
SCHOOL

MONTEREY, CALIFORNIA

THESIS

RADAR RESOURCE MANAGEMENT IN A DENSE TARGET ENVIRONMENT

by

David C. Hebert

March 2014

Thesis Advisor: Emily M. Craparo
Second Reader: W. Matthew Carlyle

Approved for public release; distribution is unlimited

THIS PAGE INTENTIONALLY LEFT BLANK

REPORT DOCUMENTATION PAGE

Form Approved OMB No. 0704–0188

1. AGENCY USE ONLY *(Leave Blank)*	2. REPORT DATE March 2014	3. REPORT TYPE AND DATES COVERED Master's Thesis	
4. TITLE AND SUBTITLE RADAR RESOURCE MANAGEMENT IN A DENSE TARGET ENVIRONMENT			**5. FUNDING NUMBERS**
6. AUTHOR(S) David C. Hebert			
7. PERFORMING ORGANIZATION NAME(S) AND ADDRESS(ES) Naval Postgraduate School Monterey, CA 93943			**8. PERFORMING ORGANIZATION REPORT NUMBER**
9. SPONSORING / MONITORING AGENCY NAME(S) AND ADDRESS(ES) N/A			**10. SPONSORING / MONITORING AGENCY REPORT NUMBER**

11. SUPPLEMENTARY NOTES

The views expressed in this document are those of the author and do not reflect the official policy or position of the Department of Defense or the U.S. Government. IRB Protocol Number: N/A.

12a. DISTRIBUTION / AVAILABILITY STATEMENT Approved for public release; distribution is unlimited	12b. DISTRIBUTION CODE

13. ABSTRACT *(maximum 200 words)*

The coordination of multifunction phased array radars across networked platforms can enable superior functionality and battle space awareness. This thesis formulates and solves a number of optimization models and heuristic algorithms to analyze and prescribe radar-to-target assignments and schedules. One optimization model uses full target information to provide a "best case" assessment of the ability of a given set of radar platforms to track a collection of targets. A modified version of this model determines the impact on these results if targets coordinate their maneuvers in order to overwhelm the radar system. We then consider the more realistic scenario in which the planner's knowledge is imperfect and describe approaches for allocating radar assets to targets in that setting. The first such approach extends an existing two-dimensional geographic allocation method to three dimensions. This allows for an allocation of the operating space to radar assets and can serve as a preallocation heuristic for more sophisticated assignment algorithms. Moreover, because the existing method does not account for transfers in tasks between geographical areas, this thesis models the additional workload involved in performing handoffs of targets between radars.

14. SUBJECT TERM optimization, radar scheduling, multifunction radar, sensor network, geographic partitioning			15. NUMBER OF PAGES 85
			16. PRICE CODE
17. SECURITY CLASSIFICATION OF REPORT Unclassified	18. SECURITY CLASSIFICATION OF THIS PAGE Unclassified	19. SECURITY CLASSIFICATION OF ABSTRACT Unclassified	20. LIMITATION OF ABSTRACT UU

THIS PAGE INTENTIONALLY LEFT BLANK

RADAR RESOURCE MANAGEMENT IN A DENSE TARGET ENVIRONMENT

David C. Hebert
Lieutenant, United States Navy
B.A., University of New Mexico, 2006

Submitted in partial fulfillment of the
requirements for the degree of

MASTER OF SCIENCE IN OPERATIONS RESEARCH

from the

NAVAL POSTGRADUATE SCHOOL
March 2014

Author: David C. Hebert

Approved by: Emily M. Craparo
                   Thesis Advisor

                   W. Matthew Carlyle
                   Second Reader

                   Dr. Robert F. Dell
                   Chair, Department of Operations Research

THIS PAGE INTENTIONALLY LEFT BLANK

ABSTRACT

The coordination of multifunction phased array radars across networked platforms can enable superior functionality and battle space awareness. This thesis formulates and solves a number of optimization models and heuristic algorithms to analyze and prescribe radar-to-target assignments and schedules. One optimization model uses full target information to provide a "best case" assessment of the ability of a given set of radar platforms to track a collection of targets. A modified version of this model determines the impact on these results if targets coordinate their maneuvers in order to overwhelm the radar system. We then consider the more realistic scenario in which the planner's knowledge is imperfect and describe approaches for allocating radar assets to targets in that setting. The first such approach extends an existing two-dimensional geographic allocation method to three dimensions. This allows for an allocation of the operating space to radar assets and can serve as a preallocation heuristic for more sophisticated assignment algorithms. Moreover, because the existing method does not account for transfers in tasks between geographical areas, this thesis models the additional workload involved in performing handoffs of targets between radars.

THIS PAGE INTENTIONALLY LEFT BLANK

Table of Contents

List of Figures

List of Tables

THIS PAGE INTENTIONALLY LEFT BLANK

List of Acronyms and Abbreviations

CEC Cooperative Engagement Capability

CTP common tactical picture

HF high frequency

HVA high value asset

IMMKF interacting multiple model Kalman filters

KF Kalman filter

LOS line of sight

LP linear programming

MFR multifunction phased array radar

MILP mixed integer linear programming

NATO North Atlantic Treaty Organization

PDF probability density function

RCS radar cross section

RTS radar task scheduler

SNR signal to noise ratio

TAS track and scan

TDL tactical data link

TWS track while scan

UAV unmanned aerial vehicle

UHF ultrahigh frequency

THIS PAGE INTENTIONALLY LEFT BLANK

Executive Summary

Advanced warships cost in excess of one billion dollars yet remain vulnerable to a single missile. The proliferation of relatively low cost and increasingly sophisticated unmanned aerial vehicles, missiles, and decoys provides our enemies the capacity to overwhelm a ship's defensive capabilities. The probability of damage from any one threat may remain low, but the success of a single missile could incapacitate a high value asset. The coordination of multifunction phased array radars across platforms is critical to obtaining superior air defense and battle space awareness during periods of high contact density. This thesis develops several models to analyze target assignments in a multiple-sensor network.

One optimization model provides a "best case" assessment of the ability of a given set of radar platforms to track a collection of targets. We assume the set of radars have perfect knowledge of the targets, including the times that each target track begins and ends and the location of the target throughout this period. This allows the model to optimize the schedule of radar observations over the entire time horizon and provides a bound for the real capabilities of a set of radars. A modified version of this model determines the impact on these results if targets coordinate their maneuvers in an attempt to exceed the resource capacity of the sensor network. Results suggest that synchronized maneuvers may produce situations where sensor resource demands exceed network capabilities. This could result in reduced track quality leading to higher track loss rates.

We also consider the more realistic scenario in which the planner's knowledge is imperfect and describe approaches for allocating sensor assets to targets based on geographic location. The first method extends an existing two-dimensional geographic allocation approach to three dimensions. By limiting the amount of the operating space we assign to a specific sensor, we develop a heuristic approach for preassigning sensors to targets that reduces the computational demands of more sophisticated assignment algorithms. In the scenarios examined, the heuristic can perform approximately 40 percent of sensor-to-target assignments with limited impact on the "best case" assessment results. This could lead to significant reductions in the real-time computations and data transfer rates required by sensor-to-target assignment algorithms.

Finally, we investigate the impact of transferring target tracking requirements between sensors by developing a model that permits the inclusion of handoff penalties. In order to do so, we modify the previously mentioned geographic allocation model by discretizing the operating space and defining target paths through this space. To account for the additional resources required when transferring a target between sensors, we assess a handoff penalty for any sensor that gains part of a target's path after it begins. For the scenario considered, we find that significant modifications to the sensors' regional assignments only occur if the resource demands for target handoffs account for more than 25 percent of the total demand.

CHAPTER 1:
INTRODUCTION

Multifunction phased array radars (MFRs) are capable of performing various tasks in rapid succession. The performance of target search, detect, and track operations concurrently with missile guidance functions allow MFRs to deliver superior battle space awareness and air defense capabilities than previously provided by multiple, single-purpose radars. Equipped with a communication network capable of sharing target data, a battle group can leverage the radar resources available on its ships to extend threat detection ranges, enhance track data, and synchronize defensive missile capabilities across platforms.

While a typical shipborne MFR can track over 100 targets independently (U.S. Navy, 2013), this could prove inadequate in a dense target environment. Combined with friendly air assets, the expanded availability of unmanned aerial vehicles (UAVs) and decoys provides the opportunity to overwhelm the tracking capacity of a single MFR with large salvos and swarm tactics. MFRs require a coordinated approach to maximize search capabilities while maintaining track quality. The multifunctional nature of modern radars complicates this process, and platform-level demands or limitations on MFRs may reduce the capacity available for coordinated search and tracking. This thesis focuses on the allocation of radar tracking requirements across multiple MFRs to reduce radar resources required for track maintenance. In this thesis, we define any radar contact as a target, including neutral and friendly air assets, to conform with the established academic lexicon.

1.1 Motivation and Background

Advanced warships cost in excess of one billion dollars yet remain vulnerable to a single missile. The proliferation of relatively low cost and increasingly sophisticated UAVs, missiles, and decoys provides the capacity to overwhelm a ship's defensive capabilities. The probability of damage from any one threat may remain low, but the success of a single missile could incapacitate a high value asset (HVA). Coordination of radar resources within a battle group can increase tracking performance during periods of high contact density. The successful integration of radar resource management across platforms relies on two critical pieces of shipboard infrastructure: MFRs and tactical data links (TDLs).

1.1.1 Phased Array Radar

MFRs consist of several elements, or antennas, spatially separated in an array. The array is designed to increase antenna gain, to allow for electronic beam formation and steering, and to determine the direction from which incoming signals arrive. In passive MFRs, a single power source provides energy to phase shifters attached to each element. When the phase of emitted radiation between individual elements is shifted, constructive interference patterns increase energy propagated in the desired beam direction while destructive interference reduces radiated energy emitted in other direction. By altering the amount of phase shift between elements, the array can direct radar beams electronically without the need to physically move any components, as illustrated in Figure 1.1.
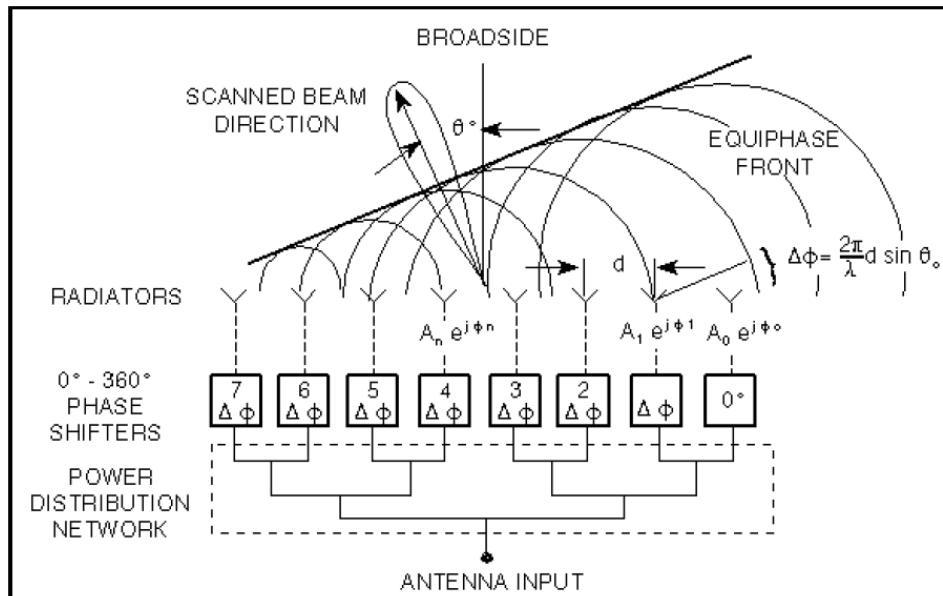
Figure 1.1: Beam steering with a linear phased array (from U.S. Navy Naval Air Systems Command, 2012, p. 3-4.3).

Unlike traditional rotating dish radars, electronic beam steering allows an MFR to cycle through tasks in various directions without delay. Thus, rather than performing "track while scan" (TWS), where radar returns obtained during a search are filtered and correlated to form tracks, MFRs more commonly operate in a "track and scan" (TAS) mode. In TAS, MFRs employ tracking beams, distinct from those generated for search, for each target

being tracked. This allows the MFR to use advanced, higher energy techniques to improve the position accuracy of targets. TAS also allows the MFR to continue to maintain tracks outside the area in which it may be performing search functions. Additionally, TAS allows the MFR to maintain different data update rates for tracking and searching. For example, where a search area may need to be covered every 10 seconds, a known target may have to be observed every second (Billiter, 1989, pp. 89–92).

While TAS allows for greater accuracy of target data, it also requires significantly more time and power from the radar than TWS. As the number of tracks increases, TAS may exceed the resources available to the MFR. The MFR can reduce this burden by using TWS to monitor long-range or low-priority targets while maintaining high-risk, high-priority targets in TAS (Billiter, 1989, pp. 93–96).

To prioritize and perform its assigned tasks, an MFR utilizes a radar task scheduler (RTS). For each time interval T_P, the RTS accepts the following inputs: a set of search beams necessary to explore the assigned search region, a track task list with the required renewal time for each track, an auxiliary task list with renewal times for each task, and the time to execute each search, track, and auxiliary task. From this input, the RTS develops a task sequence for the MFR to perform over the time interval T_P and reports any modifications to input parameters it made while developing the task sequence (Sabatini & Tarantino, 1994, pp. 219–255).

The electronic steering capability of MFRs permits the RTS to schedule several track tasks concurrently. For targets at an estimated position, the RTS can calculate the expected time between pulse transmission and a radar return. Rather than allow the MFR to idle during this delay, the RTS schedules additional tracking tasks such that the transmissions and returns for each target do not coincide. This process, known as pulse packing (Bogler, 1990, pp. 252–253) or track interleaving (Billiter, 1989, pp. 99–101), allows an MFR to update several targets during the same time required to accomplish a single tracking task.

MFRs have been in use for over three decades for aircraft surveillance and tracking (National Research Council, 2008, p. 19). Various models and variations are now installed on warships around the world. Most common on U.S. warships is the AN/SPY-1 radar. The AN/SPY-1 consists of four arrays positioned to allow 360 degree coverage. It transmits in

3

the 2 to 4 Ghz range with a peak power of 4 to 6 MW. As the primary sensor for the Aegis Weapon System, it conducts horizon and sector searches concurrently with multiple target tracking and designation (Jane's, 2012). Figure 1.2 provides an overview of AN/SPY-1 specifications and variants installed on U.S. destroyers and cruisers as well as warships from five other countries.

Attribute	SPY-1B/D	SPY-1D(V)	SPY-1F	SPY-1F(V)
Primary Ship Classes	Destroyers Cruisers Frigates	Destroyers Cruisers Frigates	Frigates Destroyers Amphibs Carriers	Frigates Destroyers Amphibs Carriers
Antenna Diameter	12 ft. (3.7 m)	12 ft. (3.7 m)	8 ft. (2.4 m)	8 ft. (2.4 m)
No. of Elements	4,350	4,350	1,856	1,856
SM-2 and ESSM Capable	Yes	Yes	Yes	Yes
All-Weather Performance	Yes	Yes	Yes	Yes
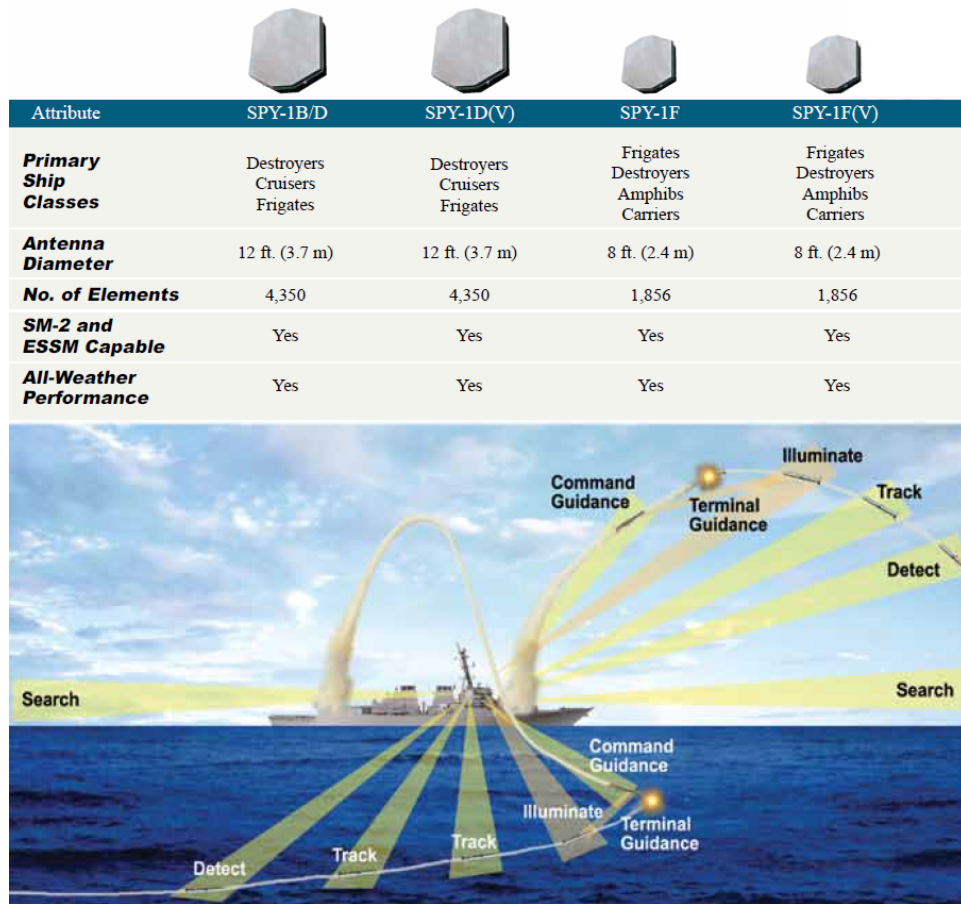
Figure 1.2: AN/SPY-1 variants (from Lockheed Martin, 2009).

1.1.2 Tactical Data Links

To develop and maintain a common tactical picture (CTP) among components of a battle group, networked platforms must be able to distribute information from each sensor in near real time. Tactical data links (TDLs) provide this capability. A TDL is an electronic connection between military platforms that allows for the transfer of digital information.

4

TDLs typically employ radio communications and transmit in the high frequency (HF) or ultrahigh frequency (UHF) range. Standardized message formats allow for encrypted direct communication between computerized tactical data systems at high data rates (Hura et al., 2000, pp. 107–121). The two primary TDLs in use by North Atlantic Treaty Organization (NATO) forces are Link-11 and Link-16.

Link-16 is the primary TDL for the distribution of situational awareness information. It uses UHF line-of-sight (LOS) transceivers to establish a network capable of data rates up to 238 kilobits/sec. Link-11 has a relatively low data rate of 1200 bits/sec, but operates over both HF and UHF, allowing for communications beyond LOS (U.S. Army, 2000). Link-22 is currently under development as a replacement for Link-11, providing greater data rates and a more stable connection over a secure, beyond-LOS TDL.

These TDLs allow radar track data such as position, heading, speed, and identification to be shared across platforms at rates up to 4,000 tracks per second (Jane's, 2011). The tracks held by each platform are compared to determine which tracks correspond to the same target. The radar tracking system automatically correlates tracks that it determines are monitoring the same target. It then combines the tracks and all available information into a single fused track. This process has proven effective, but advances in processor speeds and TDL data rates provide the opportunity to achieve a superior tactical picture through the Cooperative Engagement Capability (CEC).

Cooperative Engagement Capability

Rather than transmit processed track data, CEC allows distributed sensors to share unfiltered measurements from each observation, such as range, bearing, and elevation. TDLs distribute these measurements throughout the battle group within microseconds, allowing each unit to utilize the data as if it were provided by onboard sensors. With each platform performing the same tracking algorithm on all available data, an identical CTP is available to each CEC platform (Johns Hopkins Applied Physics Lab, 1995). As Figure 1.3 illustrates, combining radar measurement data to produce composite tracks results in a more accurate contact picture than is possible from correlating multiple tracks across platforms.
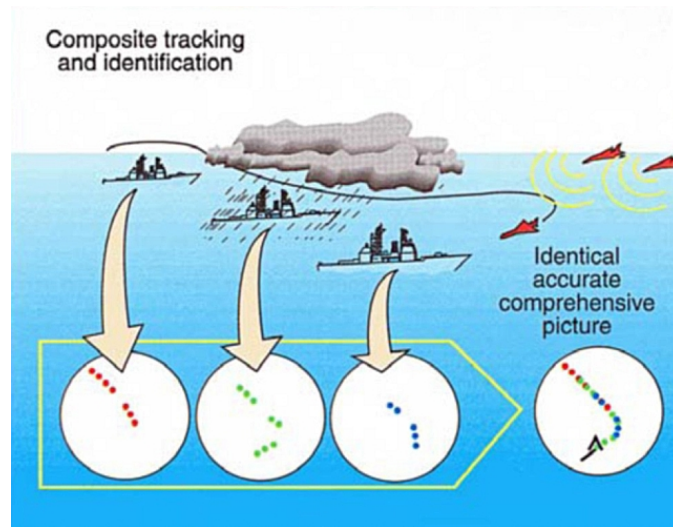
Figure 1.3: Composite tracking with CEC (from Johns Hopkins Applied Physics Lab, 1995, p. 379).

1.2 Literature Review

The problems associated with correlating multiple-target tracking across multiple sensors are well documented and analyzed. Bar-Shalom and Li (1995) provide an overview of many of the principles and techniques developed to address this topic. With the deployment of MFRs connected by high speed TDLs in the 1980s, the coordinated management of finite sensor resources to track an increasing number of targets became an active topic of research.

1.2.1 Centralized Control of Radar Resource Management

The majority of radar resource management literature focuses on the scheduling and tasking of a single sensor, such as in Bogler (1990) and Blackman (1986). Many of the techniques developed are feasible in multiple-radar environments controlled by a central scheduler, though data sharing rates limit the feasibility of their implementation. Most early research on resource management for multiple radars utilizes a centralized control element to assign tasks to networked sensors based on task priorities and the sensors' reported constraints and capabilities. Nash (1977) provides an early example of such approaches.

Given "a set of previously acquired and externally prioritized surveillance targets," Nash presents an algorithm for the optimal allocation of targets to multiple sensors during the next time step. To do so, he utilizes the classic transportation problem from linear programming (LP) which schedules the delivery of commodities from supply centers to customers at minimal cost to the system. In this case, the algorithm assigns sensors to targets in order to minimize the total cost incurred over the next time step. Costs are defined as a function of a target's priority and the estimated track accuracy obtained from the sensor assignment. Track assignments are limited by the maximum track capacity of each sensor. Nash modifies the basic transportation problem to allow more than one sensor to track a target. A benefit of using a version of the transportation problem is the availability of fast, heuristic approaches that allow for near real time calculations. Another benefit of this approach is the ability to modify sensor allocation constraints, such as by specifying target assignments or modeling reduced capacity.

The algorithm provided by Nash is step-wise optimal when the assumptions of independence and linearity of track to sensor assignment costs hold. Unfortunately, this greedy approach does not imply optimality over the total time frame of observations. Since the formulation optimizes the gains obtained over the next time step vice all future time steps, a suboptimal allocation of tracking resources may occur. The author acknowledges this limitation, but suggests one can find a globally optimal solution by integrating the formulation within a dynamic programming process.

Schmaedeke (1993) revisits this formulation, but calculates the predicted gains from sensor-to-target assignments with data available from the Kalman filter (KF). The KF is a recursive algorithm for estimating a target's physical state based on a series of measurements over time. For each observation, the algorithm updates a multivariate distribution for each state variable being tracked. As a means of measuring the potential benefits of sensor assignments, the KF provides a measure of the information content in a target's probability density function (PDF). Since it is possible to calculate the updated PDF *a priori* when using a KF, the information content of a target's PDF after the next time step can be calculated for each possible sensor assignment. Using the LP formulation developed by Nash (1977), one can determine the optimal sensor assignments. McIntyre and Hintz (1996) describe a search and track computer simulation that demonstrates the benefits of this approach over

random sensor-to-target assignments.

By defining track accuracy estimates directly from the KF, Schmaedeke provides a rational and concrete means of determining the benefits provided by sensor to target assignments. However, suboptimal allocation of resources may still occur due to the formulation's step-wise approach. Furthermore, defining the information content with the KF introduces additional restrictions. The functions developed do not provide for prioritizing targets or weighting a target's state variables when deciding the value of information gained from sensor assignment. Additionally, for a traditional KF, the calculated information gain is unaffected by target maneuvers. To increase the value assigned to observations of maneuvering targets, Schmaedeke and Kastella (1998) recommend replacing the KF with interacting multiple model Kalman filters (IMMKF). By tracking and weighting several KF motion models continuously, the IMMKF provides a computationally intensive but more robust track estimate. During maneuvers, there is greater uncertainty as to which of the KF models is accurately tracking the target. This results in a reduction of the information content present in the IMMKF model. Thus, the possible information gain from a sensor assignment increases. This makes sensor assignment to maneuvering targets more valuable and thus more likely to occur.

Rather than rely on the strict calculation of information gain prescribed by Schmaedeke and Kastella (1998), Blackman (1986, pp. 397–401) suggests employing utility theory to determine sensor allocation. To maximize overall utility, the algorithm calculates the marginal utility of assigning a sensor to a given track for each possible pairing. The utility of a target's track depends on the value placed on different levels of track accuracy. The marginal utility is the difference in expected utility after the next time step with or without the sensor to target assignment. The system designer can control the shape of the utility function to ensure sensor assignments only add significantly to the marginal utility if they provide actionable level target accuracy. The marginal utility is also dependent on the weighted probabilities of a target's type and threat assessment, both before and after sensor assignment. After calculating the marginal utility for each sensor-target pair, an optimal assignment algorithm appoints sensors to targets. Unlike the approach presented by Nash, Blackman's approach requires a one-to-one assignment of sensors to targets, which prohibits its direct application to real world tracking problems.

Veeramachaneni and Osadciw (2006) shift the focus from optimizing the next scheduled observation time to a more comprehensive approach for multiple sensor resource allocation. Rather than optimizing a target's track accuracy, they focus on the allocation of available radar dwell time and energy between search and track functions for a sensor network. The objective function is the weighted sum of two competing objectives: the search coverage area and the probability of detection of tracked targets. Each time the target picture transforms, the controlling element must resolve the problem and reassign the radars. To approach an optimal solution in near real time, the authors suggest implementation of a particle swarm optimization algorithm (Eberhart & Kennedy, 1995). While this heuristic approach does not guarantee optimality, it does allow for continuously updated solutions to provide a best known allocation of time and energy in near real time situations.

To overcome the limitations of step-wise optimal assignments, this thesis begins by assuming universal knowledge of targets. This includes knowledge of when the sensor network gains and loses a track and the target positions during this timeframe. This assumption provides the ability to determine an optimal observation schedule for each target that minimizes the use of radar resources over the entire timeframe considered. While this is not a feasible approach for real radar scheduling, it does provide a "best case" bound on the resources required to maintain a given track picture. We relax this assumption later in the thesis when we investigate geographical partitioning methods. Unlike Veeramachaneni and Osadciw, this thesis assumes there is a specified amount of radar resources available for tracking. For simplification, we do not analyze the interrelationship of tracking capacity with other radar functions.

1.2.2 Distributed Control of Radar Resource Management

While centralized radar resource management techniques can provide optimal solutions, data sharing rates and computation speeds limit their feasibility in a distributed sensor network. Recent research attempts to overcome these technical limitations by developing decentralized decision making algorithms. By developing distributed solutions that can approach optimality over time, the algorithms provide actionable decisions even when communications are limited.

Dorman, Leung, Nicholson, Siva, and Williams (2005) suggest two decentralized decision

making algorithms for sensor to target assignments and weapon allocations based on information theory. The first expands on the approach developed by Nash (1977). Instead of delivering all cost and threat data to a central planner to solve the LP problem and distribute target assignments, the network distributes the necessary data to all platforms which independently solve the LP to determine the targets for which they are responsible. While this approach can guarantee optimality within a tactical time frame for many networks, delays in data sharing can prevent the algorithm from reaching an optimal solution.

To reduce the volume of data shared between platforms, Dormon et al. (2005) developed a second algorithm based on a decentralized auction. Rather than transfer all cost and threat data between each set of platforms, sensors only exchange one bid for each target. By limiting the information that must be shared, this algorithm reduces the possibility of exceeding a network's data transfer capacity. The bids are used by each platform to run the decentralized auction algorithm independently and determine the optimal target assignments. The current framework for target data fusion across TDLs could allow these bids to be distributed by slightly reformatting the standardized target messages. This would limit the additional throughput capacity required for implementation and ensure the algorithm is scalable for situations with greater target density.

Additional approaches to decentralized decision making rely on self-organization processes. Self-organization, or emergent behavior, is a process where meaningful global patterns emerge from the interactions of simple agents with each other and their local environment using only local information and without any centralized control (Camazine et al., 2001, pp. 7–8). For radar networks, the agents are sensor schedulers and the local environment is the shared track picture. Stigmergy, a subset of self-organization in which agents only interact indirectly with one another through their impact on the environment, underlies the resource management approaches proposed in Weir and Sokol (2009) and Lambert and Sinno (2011).

Weir and Sokol (2009) suggest local decision rules for radar management based on data from a shared track file. These rules result in global patterns consistent with optimal results obtained from centralized control. To determine which tracks should be observed over the upcoming time period, each platform independently develops scores for each target based on potential track accuracy improvements. The proposed scoring function is dependent on

the track state, track error covariance, range, and measurement uncertainties. Each sensor ranks the tracks to ensure the most effective observations happen first. Following these observations, the platforms update their shared track picture and score and rank the targets again. Appropriate local scoring criteria result in radar resource decisions that approach optimal solutions without central decision making or direct interaction between platforms.

Beyond the potential to approach optimal resource allocation, Weir and Sokol (2010) also demonstrate that self-organizing radar managers react rationally to network degradations. When disruptions to network capabilities occur, the radars return to optimal decisions for independent operations. If one sensor loses communication with the network, the same local scoring criteria adapt to the new network configuration and radar resource decisions approach optimality over time.

Rather than focus on a sensor's potential impact on the future track picture, Lambert and Sinno (2011) develop local rules for resource allocation based on the information gain achieved for a given target during previous observations. Though radars do not interact directly in stigmergic systems, they can sense the impact of others through their environment. By comparing the local information gain to the global information gain for an observed target, a radar can assess how important its contribution is to the global track picture. If the local information gain is significantly smaller than that observed in the global track file, Lambert and Sinno suggest measures to induce the radar to focus on other targets for which it may have a greater impact.

These algorithms developed for distributed control of resources still require a significant amount of data transfer and computational effort each time sensor-to-target assignments are optimized. A portion of this thesis investigates the effect of assigning sensors to targets based on geographic location. The minimal computational requirements of this method are conducive to real time implementation. However, reliance on geographic partitioning alone oversimplifies the problem, leading to periods where sensors lack the resources to adequately monitor their assigned targets. While not a replacement for the approaches mentioned in this section, the assignment methods developed in this thesis may be able to reduce the real time computational demands of these algorithms by reducing the problem size.

1.3 Problem Statement and Assumptions

This thesis investigates how to manage a distributed network of radar assets when operating in a dense target environment. Several factors complicate the optimal use of available radar resources. The multifunctional nature of modern radars places demands on resources often not known to the network. Furthermore, multiple objectives exist when scheduling radar resources, namely minimizing emitted power and dwell time. Optimization of one of these does not necessarily result in optimal or near optimal results for the other. To continue exploring this problem, we focus solely on the tracking function of MFRs and make some simplifying assumptions.

To remove directional and environmental effects, we assume variations in sensor effectiveness only depend on range and emitted power. That is, we do not consider the complex effects of weather, land objects, and the directional limitations of MFR arrays on radar tracking. We also assume that all targets have identical tracking requirements; that is, we do not attempt to utilize knowledge of targets to prioritize them by threat levels. The sensor-to-target assignment models in this thesis do not rely on these assumptions, but the scenarios considered in our analysis comply with them. These assumptions are necessary for the partitioning models presented.

Common to all models, we assume that any radar return above a signal to noise ratio (SNR) threshold of 13 dB provides the same information gain to the sensor network. This means that there are no false positive or false negative returns, that the radar assigns each return correctly to its track, and that the resultant track quality after any observation is equivalent. Finally, we assume that track data is distributed to all sensors by the TDL without time delay and unrestricted by throughput capacity.

This thesis is organized as follows. Chapter 2 introduces an optimal radar to target assignment model that provides a best-case radar schedule for networked MFRs. We extend this model to allow for analysis of the potential difficulties introduced to the radar scheduling process by the coordinated maneuvers of targets. Chapter 3 introduces an optimal partitioning model for assigning tracking requirements to sensors based on the geographic location of targets. We also present two variations to this model. The first permits regions of space to remain unassigned, allowing any sensor to perform tracking in these regions. The sec-

ond accounts for the potential difficulties of handing off targets between sensors. Chapter 4 presents the analysis performed using each of these models, and Chapter 5 provides a conclusion and recommendations for further research.

THIS PAGE INTENTIONALLY LEFT BLANK

CHAPTER 2:
OPTIMAL RADAR ASSIGNMENT IN A KNOWN
TARGET ENVIRONMENT

In this chapter, we investigate the performance bounds of networked sensors. Specifically, we develop a model to determine the best use of radar resources when multiple MFRs coordinate through an infinite-capacity network with zero time delay. We consider an environment in which the sensor scheduler has universal knowledge of each target's locations and maneuvers over the period of time tracking occurs. Eliminating the uncertainty in future events allows the scheduler to optimally allocate resources over the entire period of interest. While this algorithm is not deployable as a real-world radar scheduling technique, it does provide a best-case bound to which one can compare other algorithms.

2.1   Multifunction Radar Capabilities

For a radar to recognize a return from a target, the signal to noise ratio (SNR) of the target echo must exceed an established threshold. A number of factors effect how much of a radar's emitted energy is sensed by the radar receiver. External variables, such as the target's range and environmental noise, as well as internal factors, such as antenna gain and electrical losses, effect how strong the radar signal is compared to all sources of noise. Equation (2.1) is a reproduction of the radar equation provided in Sabatini and Tarantino (1994, p. 27). Each factor presented, whether controlled by the radar or not, can impact the SNR.

$$SNR = \frac{P^{trans}G^{trans}G^{rec}\lambda^2 F^{trans}F^{rec2}\sigma^o}{(4\pi)^3 R^4 k_0 T_0 F^n L^{tot}}\tau \tag{2.1}$$

where

P^{trans} =   Transmitted power [MW]

G^{trans} =   Transmitter antenna gain in the direction of the target [dimensionless]

G^{rec} =   Receiver antenna gain in the direction of the target [dimensionless]

λ	=	Transmit wavelength [cm]
F^{trans}	=	Transmitter propagation factor [dimensionless]
F^{rec}	=	Receiver propagation factor [dimensionless]
σ^o	=	Target radar cross section (RCS) [m^2]
R	=	Range to the target [m]
k_o	=	Boltzmann constant [$1.38x10^{-23}$J/K]
T_o	=	Standard Temperature [290 K]
F^n	=	Receiver noise figure [dimensionless]
L^{tot}	=	Total losses for the radar system [dimensionless]
τ	=	Radar pulse width [μsec]

Table 2.1 provides values for the variables in Equation (2.1) derived from the benchmark problem for phased array radars developed in Blair and Watson (1996). The radar cross section (RCS) of all targets is established as one square meter for simplification, but the following formulations are not limited to this value or to a constant RCS throughout the trajectory of the targets. Blair and Watson establish eight discrete waveforms available for use with varying radar pulse widths, τ_k.

P^{trans}	1 MW
G^{trans}	4752
G^{rec}	4752
λ	7.5 cm
F^{trans}	1
F^{rec}	1
σ^o	1 m
F^n	2
L^{tot}	144.5

No.	τ (μsec)
1	1.35
2	2.25
3	4.05
4	5.85
5	11.70
6	23.40
7	46.8
8	93.6

Table 2.1: Radar parameters and pulse width options (after Blair and Watson 1996).

The radar pulse width must be long enough to ensure adequate energy is emitted to obtain an SNR above the sensor's threshold. We assume that an SNR above 13 dB provides perfect

detection without false alarms. Furthermore, we assume that any SNR above the threshold results in the same track accuracy and requires the same update rate. Thus, the radar utilizes the waveform that meets the SNR threshold with the least emitted energy.

2.2 Sensor-to-Target Assignment Model

We now describe a model that optimizes the schedule of observations required from networked sensors for a given set of tracks. For this model, we make the additional assumption that we have prior knowledge of each track's duration and location. This allows the model to determine the optimal schedule over the entire time horizon. To limit computational effort, we establish a dynamic set of waveforms from each sensor that are available for observing each target at each time step. Since we assume each observation provides the same information gain, the set only contains the waveform from each sensor that meets the SNR threshold with the least emitted energy.

Decision variables $X_{i,j,t,k}$ describe the optimal scheduling of track observations by sensors to minimize the amount of power and time invested in tracking and limit the impact of delays due to radar resource limitations. We assume that longer time delays result in a continued reduction in track quality and an increasing probability of track loss. The model utilizes multiple linear constraints to capture this nonlinear impact on the quality of a tracking schedule. This ensures the model limits both the total time of all delays and the length of those delays.

2.2.1 Formulation

Index Use [˜Cardinality]

$t \in T$	time steps [˜100]
$i \in I$	sensors [˜3]
$j \in J$	targets [˜30]
$k \in K$	waveforms [˜8]
$l \in L$	time steps during the required observation interval $|L|$ [˜10]
$n \in N$	segments of a piece-wise linear delay penalty function[˜2]
$(j,t) \in M \subset J \times T$	time steps t in which target j is tracked [˜3000]

Given Data [Units]

τ_k pulse width of waveform k [μsec]

$p_{transmit}$ transmitter power [MW]

$interleave\_limit$ number of targets a sensor can observe per time step [targets]

m_n slope for penalty constraint n [J]

b_n intercept for penalty constraint n [J]

Calculated Data [~Cardinality]

$(i,j,t,k) \in P \subset I \times M \times K$ set of waveforms k from sensor i that are capable of obtaining an SNR above the threshold SNR_{min} for target j at time t with the least emitted energy [~9000]

$$P = \left\{ (i,j,t,k) | (j,t) \in M \text{ and} \right.$$
$$\left. k = \arg\min_k \left(\tau_k \left| \frac{P_k^{trans} G_{i,j,t}^{trans} G_{i,j,t}^{rec} \lambda^2 F_{i,j,t}^{trans} F_{i,j,t}^{rec2} \sigma_{i,j,t}^o}{(4\pi)^3 R_{i,j,t}^4 k_0 T_0 F_i^n L_{i,j,t}^{tot}} \tau_k \geq SNR_{min} \right) \right\} \right.$$

Decision Variables [Units]

$X_{i,j,t,k}$ binary decision to observe target j with sensor i at time t with waveform k [binary]

$NO\_LOOK_{j,t}$ binary decision to miss required observation of target j between times $t+1$ and $t+|L|$ [binary]

$DELAY_{j,t}$ number of time steps by which an observation of target j has been delayed as of time $t+|L|+1$ according to the observation frequency requirement [time steps]

$DELAY\_PENALTY_{j,t}$ penalty for number of time steps that an observation of target j at time $t+|L|+1$ is delayed beyond the required observation interval $|L|$ [J]

Formulation

$$\min_{\substack{X, \\ NO\_LOOK, \\ DELAY, \\ DELAY\_PENALTY}} \sum_{(i,j,t,k)\in P} \left(p_{transmit}(\tau_k - \frac{\tau_1}{t})X_{i,j,t,k} \right) + \sum_{(j,t)\in M} DELAY\_PENALTY_{j,t} \quad (2.2)$$

s.t.

$$\sum_{j,k:(i,j,t,k)\in P} X_{i,j,t,k} \leq interleave\_limit \qquad\qquad \forall i,t \quad (2.3)$$

$$\sum_{l,i,k:(i,j,t,k)\in P} X_{i,j,t+l,k} + NO\_LOOK_{j,t} \geq 1 \qquad\qquad \forall(j,t) \in M \quad (2.4)$$

$$DELAY_{j,t} - DELAY_{j,t-1} \geq 1 - (1 - NO\_LOOK_{j,t})t \qquad \forall(j,t) \in M \quad (2.5)$$

$$DELAY\_PENALTY_{j,t} \geq m_n(DELAY_{j,t} - DELAY_{j,t+1}) + b_n \qquad \forall n, (j,t) \in M \quad (2.6)$$

$$NO\_LOOK_{j,t}, DELAY_{j,t}, DELAY\_PENALTY_{j,t} \geq 0 \qquad \forall(j,t) \in M \quad (2.7)$$

$$X_{i,j,t,k} \in \{0,1\} \qquad\qquad \forall(i,j,t,k) \in P \quad (2.8)$$

2.2.2 Discussion

The objective function (2.2) expresses the total cost of a solution as the sum of the energy transmitted and the penalties for delaying observations of a target. To eliminate multiple optimal solutions and reduce computational time, the objective includes the factor $\frac{\tau_1}{t}$ to force sensor observations to occur as early as possible without requiring additional observations or more costly waveforms. $DELAY\_PENALTY_{j,t}$ models a piecewise linear, convex penalty function that is large enough to ensure an observation is performed, if possible, rather than accept the penalty.

Each constraint (2.3) prevents the scheduling of observations by a single sensor at a given time in excess of the interleaving limit. To ensure each target is monitored at the required sampling frequency, each constraint (2.4) requires at least one observation to occur within $|L|$ time steps of t or records the missed observation.

Constraints (2.5) and (2.6) combine to calculate the penalty for delaying observations. Constraints (2.5) determine the amount of time by which observations of target j are delayed

19

at time $t + |L|$. If $NO\_LOOK_{j,t}$ is zero, then $DELAY_{j,t}$ is zero. Otherwise, $DELAY_{j,t}$ is the number of consecutive time steps $NO\_LOOK_{j,t}$ has been equal to one up to time t. Constraints (2.6) utilize $DELAY_{j,t}$ to calculate the penalty for delaying observations. The constraints only assess a penalty for the time that a delayed observation actually occurs. For those time steps with a delayed observation, the difference between consecutive $DELAY_{j,t}$ is equivalent to the number of time steps that the schedule delays the observation. As Figure 2.1 illustrates, multiple linear constraints combine to obtain a non-linear penalty response. This causes one long delay to be more expensive than multiple shorter delays of the same total length. Table 2.2 provides an example of the calculations performed by constraints (2.5) and (2.6). Constraints (2.7) and (2.8) define the domains of the decision variables.
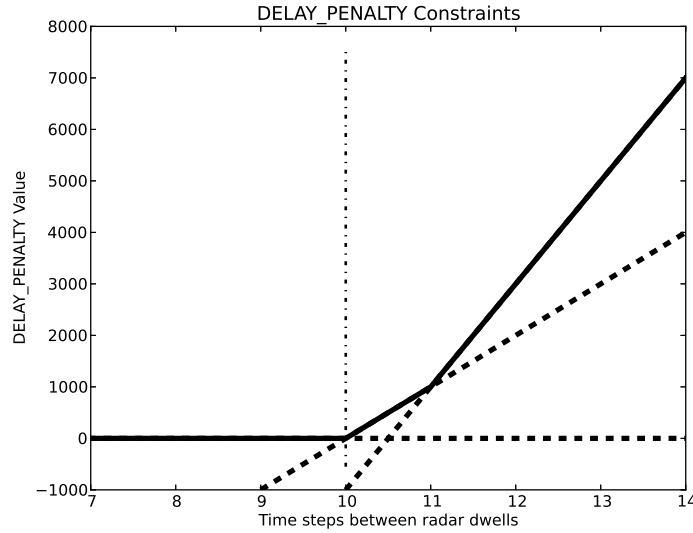

Figure 2.1: Delay penalty constraints.

t	$\cdots$	14	15	16	17	18	19	$\cdots$
$NO\_LOOK_{j,t}$	$\cdots$	0	0	1	1	1	0	$\cdots$
$DELAY_{j,t}$	$\cdots$	0	0	1	2	3	0	$\cdots$
$DELAY\_PENALTY_{j,t}$	$\cdots$	0	0	0	0	5000	0	$\cdots$

Table 2.2: Notional delay penalty calculation.

20

Figure 2.2 provides a geographical representation of results from the sensor-to-target assignment model for a network of three sensors maintaining 20 tracks. The sensors, represented by circles, are stationary throughout the problem and the targets, represented by black arrows, move along their predetermined tracks at constant speed and direction. The hash marks are observations along the targets' paths. The size and color of the hash marks correspond to the power utilized and the sensor performing the observation, respectively.
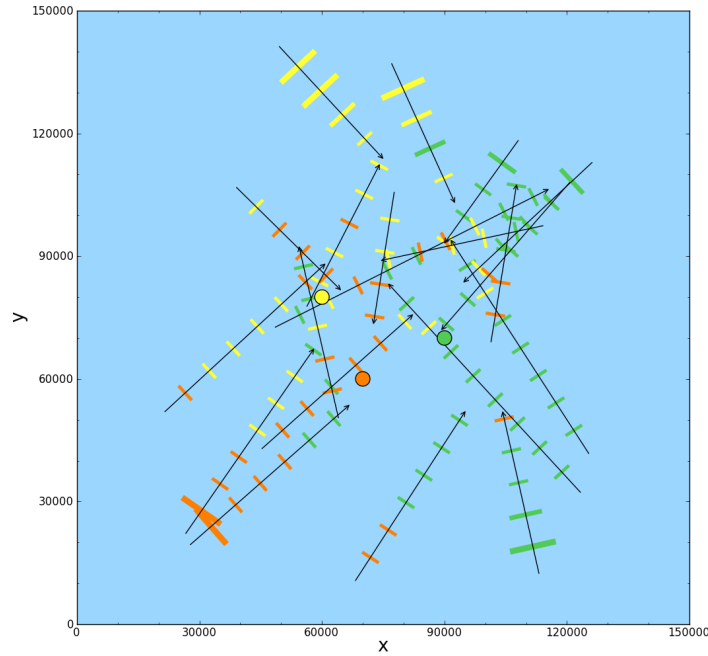

Figure 2.2: Geographic display of results for scenario involving three sensors and 20 targets.

Figure 2.3 (a) provides a timeline of the results presented in Figure 2.2. For this example, the *interleave_limit* is set to one, constraining each sensor to observe at most one target per time period. The observation frequency $|L|$ is 10 time steps. Figure 2.3 (b) displays the power requirements for each sensor to execute the optimal observation schedule as a running average over 10 time steps.
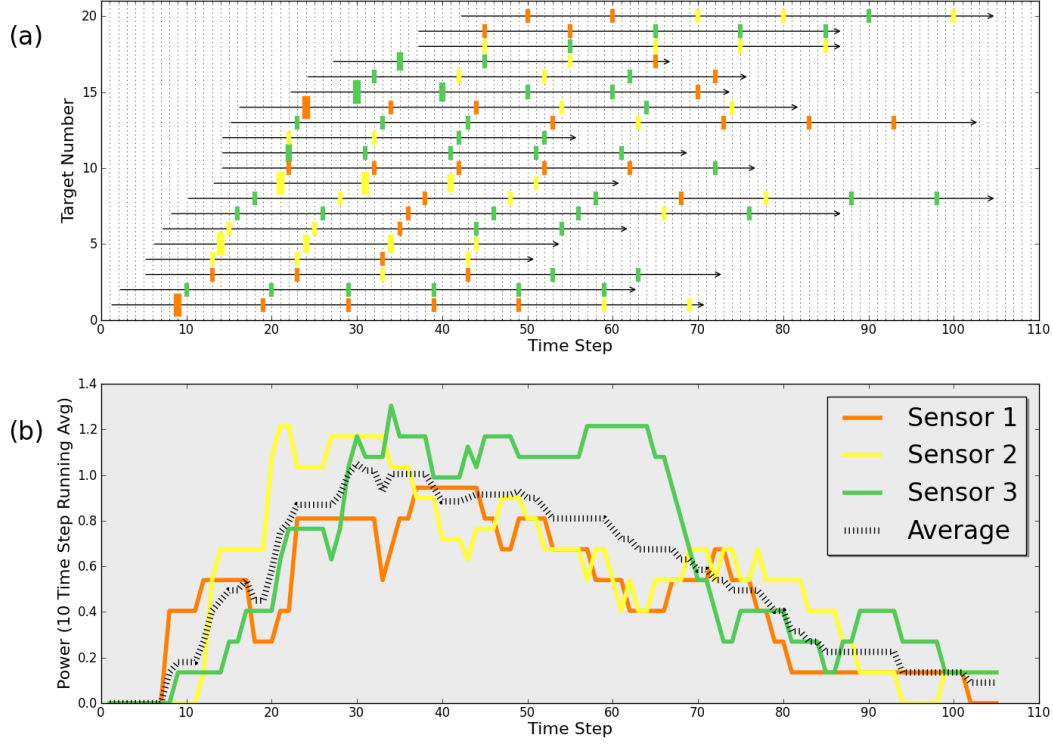
Figure 2.3: Timeline and power demands of optimal results for scenario involving three sensors and 20 targets.

2.3 Maneuverable Targets

To investigate the potential effects of airborne adversaries capable of coordinating their operations, we extend the sensor-to-target assignment model to allow for target maneuvers. Following a target maneuver, the sensor network must perform additional observations to account for the reduction in track accuracy. To model this, we declare the subset $(j,t) \in Q \subset M$ to define the time t that target j maneuvers. We then increase the number of observations required during the period of length $|L|$ immediately following the maneuver. For each of the observations following a maneuver that the sensor network is unable to schedule, the formulation assesses a penalty.

2.3.1 Formulation

In addition to the indices, data, and variables described in Section 2.2, we introduce the following nomenclature.

Index Use [~Cardinality]

$(j,t) \in Q \subset M$ time step t at which target j maneuvers [~30]

Given Data [Units]

turn_looks   number of observations required during normal observation frequency $|L|$ following a target maneuver [observations]

turn_penalty   penalty for number of observations missed following a target maneuver [J/observation]

Decision Variables [Units]

$MISSED\_LOOKS_j$ number of required observations missed following the maneuver of target j [observations]

Formulation

$$\min_{\substack{X, NO\_LOOK, \\ DELAY, \\ DELAY\_PENALTY, \\ MISSED\_LOOKS_j}} \sum_{(i,j,t,k) \in P} \left(p_{transmit}(\tau_k - \frac{\tau_1}{t}) X_{i,j,t,k} \right) + \sum_{(j,t) \in Q} DELAY\_PENALTY_{j,t}$$

$$+ turn\_penalty \sum_j MISSED\_LOOKS_j$$

$$(2.9)$$

23

s.t.

$$\sum_{(l,i,k,t):(j,t)\in Q \text{ and } (i,j,t,k)\in P} X_{i,j,t+l,k} + MISSED\_LOOKS_j \geq turn\_looks \qquad \forall j$$

(2.10)

$$\sum_{(j,k):(i,j,t,k)\in P} X_{i,j,t,k} \leq interleave\_limit \qquad \forall i,t$$

(2.11)

$$\sum_{(l,i,k):(i,j,t,k)\in P} X_{i,j,t+l,k} + NO\_LOOK_{j,t} \geq 1 \qquad \forall (j,t) \in M$$

(2.12)

$$DELAY_{j,t} - DELAY_{j,t-1} \geq 1 - (1 - NO\_LOOK_{j,t})t \qquad \forall (j,t) \in M$$

(2.13)

$$DELAY\_PENALTY_{j,t} \geq m_n(DELAY_{j,t} - DELAY_{j,t+1}) + b_n \qquad \forall n, (j,t) \in M$$

(2.14)

$$NO\_LOOK_{j,t}, DELAY_{j,t}, DELAY\_PENALTY_{j,t} \geq 0 \qquad \forall (j,t) \in M$$

(2.15)

$$MISSED\_LOOKS_j \geq 0 \qquad \forall (j,t) \in M$$

(2.16)

$$X_{i,j,t,k} \in \{0,1\} \qquad \forall i, (j,t) \in M, k$$

(2.17)

2.3.2 Discussion

The objective function (2.9) expresses the total cost of a solution as the sum of the energy transmitted and the penalties for delaying or missing observations on a target. It is similar to the objective function (2.2) from Section 2.1 with one additional component. $turn\_penalty\sum_{j}MISSED\_LOOKS_j$ penalizes a solution for failing to perform the additional observations required following a target's maneuver. As with $DELAY\_PENALTY_{j,t}$, the $turn\_penalty$ is large enough to ensure observations are performed, if feasible, rather than accept the penalty.

Constraints (2.10) reflect the required *turn_looks* during the period $|L|$ following a maneuver by target j at time t. Each additional observation that the set of sensors fails to schedule during this timeframe is tallied as *MISSED_LOOKS$_j$*. Constraints (2.11) prevent the scheduling of observations by a single sensor at a given time in excess of the interleaving limit. To ensure each target is monitored at the required non-maneuvering sampling frequency, each constraint (2.12) requires at least one observation to occur within $|L|$ time steps of t or record the missed observation.

Constraints (2.13) and (2.14) combine to calculate the penalty for delaying observations and are identical to constraints (2.5) and (2.6) discussed in Section 2.2.2. Constraints (2.15),(2.16) and (2.17) define the domains of the decision variables.

The computational requirements of this problem preclude an exhaustive analysis of networks of significant size or complexity. In an attempt to reduce the computational effort, we developed an attacker-defender model that allowed for one maneuver per target over the time horizon. The formulation failed to provide computational benefits because the solver had to execute the subproblem for each possible maneuver schedule before obtaining optimal results. To remove the unnecessary calculations of maneuver schemes, we instead iterated through every feasible combination of maneuvers for the targets to determine the "worst case" set of maneuvers.

For simplification, we maintain the assumption that each target may perform at most one maneuver during the planning horizon. Furthermore, for each time step, we assume there is only one maneuver available to each target being tracked. For example, at any time step, a target only has the option to turn 90 to the right. Figure 2.4 displays the schedule obtained following the "worst case" maneuvers for a scenario with two sensors and six targets arriving every two time steps. The time horizon for this scenario is 20 time steps. The sensors must observe each target at least once every three time steps. Following a target maneuver, three observations must occur within the next three time steps or a penalty is assessed. We allow for target maneuvers any time from one time step after target tracking begins to three time steps before the target track terminates. By preventing later maneuvers, we ensure that the sensors have the opportunity to perform the required observations following a target maneuver. In the "worst case" maneuver scheme, the targets synchronize their maneuvers into two blocks to concentrate the tracking demands on the sensor network. The

decision of the targets to maneuver in different time blocks is a result of the varying track arrival and departure times. In this scenario, the coordinated decisions of targets result in insufficient sensor capacity to perform all required observations following maneuvers. Section 4.1 discusses additional results from this formulation.
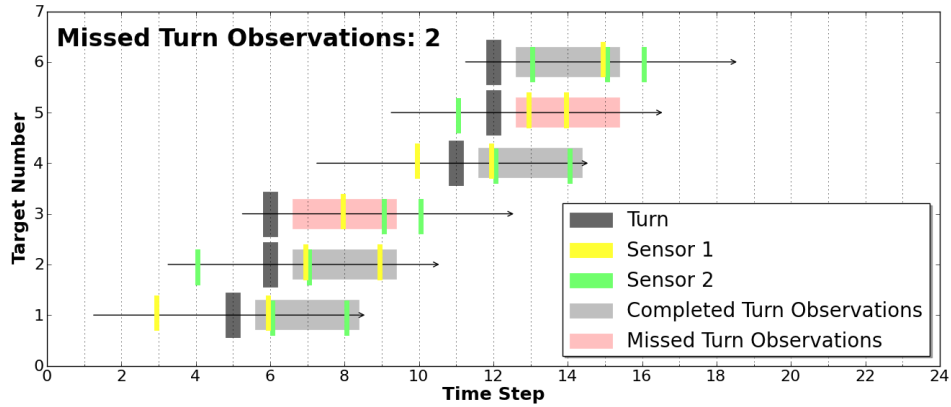

Figure 2.4: Optimal observation schedule with "worst case" maneuvers for scenario involving two sensors and six targets.

CHAPTER 3:
TARGET ALLOCATION BASED ON GEOGRAPHIC LOCATION

The formulations of Chapter 2 rely on the assumption that the sensors have perfect knowledge of the target locations and track durations. This is useful for identifying trends in the resultant schedules but prohibits the application of the model in real world situations. Interestingly, results obtained from these formulations suggest significant regions of the target operating space are often dominated by a single sensor. Figure 3.1 displays the results of 120 simulations geographically. Each simulation distributes 25 targets randomly throughout the operating space while the locations and capabilities of the three sensors remain constant. Observations indicate that a single sensor begins to dominate regions as the distance to the sensor network increases. This suggests that a target's physical position may provide enough information for a network to allocate some portion of targets to sensors.
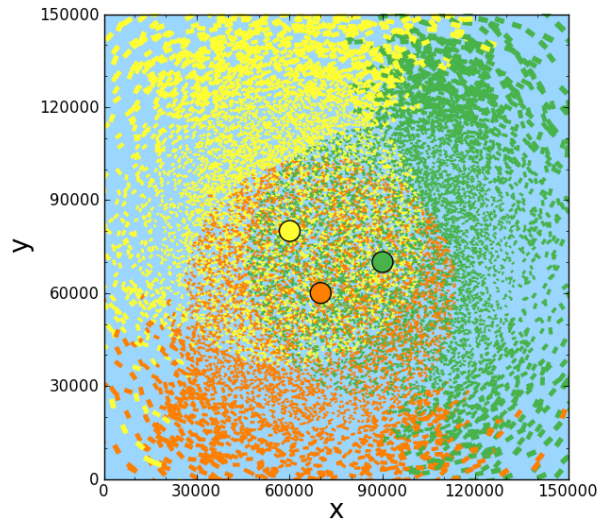

Figure 3.1: Observations from optimal schedules for 120 simulations involving three sensors and 25 targets.

27

To investigate the possibility of assigning radars to targets based on geographic location, we develop a model to partition the physical decision space so as to balance the resultant radar resource demands between sensors. This model does not rely on the assumption that sensors have perfect knowledge of the targets. Instead, it relies on an estimate of the expected target density within the operating space. To account for the increased uncertainty introduced by eliminating this assumption, we suggest a relaxation to this partitioning model that limits the amount of space assigned to a specific sensor and allows any sensor to track targets in the unassigned regions. This reduces the probability of exceeding a sensor's tracking capacity by limiting the sensor-to-target assignments prescribed based on geographic location. To investigate the impact that transferring target tracking requirements between sensors has on geographical partitioning, we develop another model to account for the increased workload inherent in target handoffs.

3.1   Geographic Assignment

To analyze the potential benefits of assigning sensors to targets geographically, we extend an optimal partitioning model developed by Carlsson (2012) to three dimensions. In addition, we adjust the formulation to account for radar power requirements, individual sensor tracking capacity, and varying target densities throughout the physical decision space.

3.1.1   Formulation

To partition space between sensors, we consider three factors. First, to observe a target at position x, a sensor must emit energy proportional to the fourth power of the range to the target, as required by Equation (2.1). Second, the assigned regions of space should be proportional to the capacity that each sensor can provide to tracking functions. Radars in a degraded status or involved heavily in other functions, such as searching or illuminating, should handle less of the tracking demands for the sensor network. Third, points in space should be weighted by the expectation of observing a target at that position during a scenario. Regions of high target density will result in proportionally greater demands on radar resources than areas of low target activity. The following mathematical formulation accounts for these factors.

Index Use [~Cardinality]

$x \in D$ positions in physical space [infinite]

$i \in I$ sensors [~3]

Given Data [Units]

α_i relative capacity of sensor i to conduct tracking [energy/target/dist^4]

$\rho(x)$ expected density of targets evaluated at position x [targets/time/volume]

p_i position of sensor i [unitless]

Decision Variables [Units]

R_i region of space assigned to sensor i [unitless]

Formulation

$$\min_{R_1,\dots,R_n} \max_i \iiint\limits_{R_i} \alpha_i \rho(x) \|x - p_i\|^4 \, dV \tag{3.1}$$

s.t.

$$\bigcup_{i=1}^n R_i = D \tag{3.2}$$

3.1.2   Discussion

The objective function (3.1) minimizes the maximum demand on any sensor by choosing which regions of space to assign to each sensor. The integrand accounts for the sensor and target attributes previously mentioned as critical to acquiring an optimal partition. The density function $\rho(x)$ can account for different target types by utilizing Equation (3.3).

$$\rho(x) = \sum_{j=1}^{n} \beta_j \rho_j(x) \tag{3.3}$$

Parameter β_j is a weighting for target type j to account for unique factors, such as RCS, threat level, and update requirements. The constraint (3.2) ensures all of the physical space is assigned to at least one of the sensors' regions.

3.1.3 Dual Formulation

The formulation of Section 3.1.1 permits reformulation as an infinite-dimensional mixed integer linear programming (MILP) problem. The following formulation is the dual of the LP problem obtained by relaxing the integer constraint of the MILP problem. This formulation provides a means of computing the solution to the formulation presented in Section 3.1.1 by reducing the number of decision variables to a cardinality proportional to the number of sensors. Carlsson (2012) provides the proof of duality, which is reproduced in the appendix, and a computational algorithm. Indices and given data remain consistent with Section 3.1.1.

Decision Variables [Units]

λ_i dual variable associated with sensor i [unitless]

$\sigma(x)$ dual variable for tracking sensor assignment to position x [m^4]

Formulation

$$\max_{\lambda,\sigma} \iiint_D \sigma(x) \mathrm{d}V \tag{3.4}$$

s.t.

30

$$\sigma(x) \leq \lambda_i \alpha_i \rho(x) \|x - p_i\|^4 \qquad \forall x, i \qquad (3.5)$$

$$\sum_i \lambda_i \leq 1 \qquad (3.6)$$

$$\lambda_i \geq 0 \qquad \forall i \qquad (3.7)$$

3.1.4 Dual Discussion

The dual objective function (3.4) maximizes the sum of sensor assignment costs across all space D. Constraints (3.5) bound σ at position x by the assignment costs for each sensor. Constraints (3.6) ensure the sum of all λ_i do not exceed one. Constraints (3.7) define the domains of the decision variables λ_i.

Assigning regions with Equation (3.8) results in optimal partitioning. The appendix provides an adaptation of the theorem and proof from Carlsson (2012) for our formulation. Each location x in D is assigned to sensor i only if the cost $\lambda_i \alpha_i \|x - p_i\|^4$ is less than the cost of assignment to any other sensor.

$$R_i = \left\{ x \in D \quad | \quad \lambda_i \alpha_i \|x - p_i\|^4 \leq \lambda_j \alpha_j \|x - p_j\|^4 \qquad \forall j \neq i \right\} \qquad (3.8)$$

This formulation provides several benefits for a distributed radar network. First, it permits inclusion of the critical factors established in Section 3.1.1. Second, it is scalable for the inclusion and removal of sensors. The dynamic nature of radar networks in an adverse environment requires the partitioning process to allow for changes in network size and geometry. This formulation allows for the recalculation of partitions at speeds consistent with the transitions of sensor network structures. Finally, the partitioning is adaptable to fluctuations in individual radar tracking capacity. If new demands or limitations on sensor i reduce the amount of resources available for tracking, the region assigned to that radar can be reduced proportionately by varying the value of α_i. A sensor's declaration of reduced capacity through the TDL, or a loss of communication with the network, will allow the other sensors to calculate their newly assigned regions.

Figure 3.2 displays an expected target density function $\rho(x)$ for a three dimensional scenario with a single HVA and three directions of approach for targets. Three networked sensors are positioned between the HVA and the threat axes. Applying the geographic partitioning model, each sensor is assigned the regions displayed in Figure 3.3.
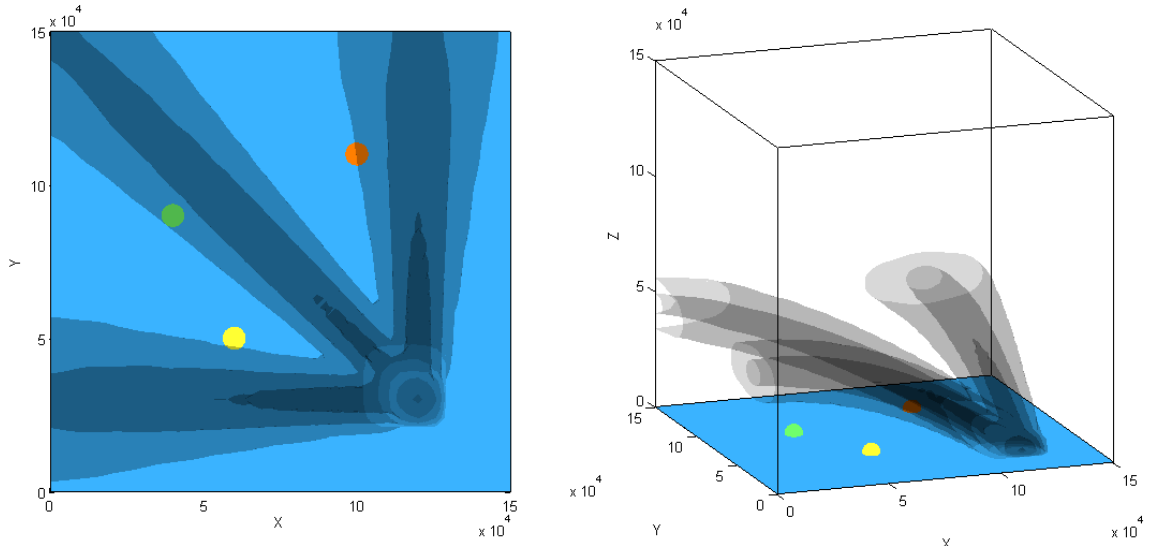

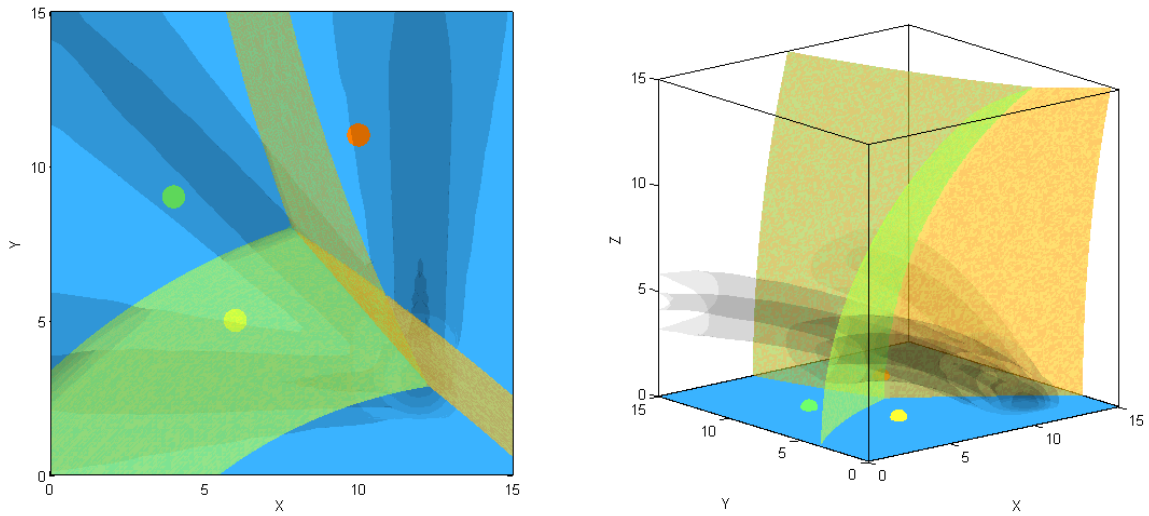Figure 3.2: Three dimensional target density for one HVA with three directions of approach.

Figure 3.3: Optimal partition of space for target density in Figure 3.2.

3.2 Relaxation of Geographic Assignment

By partitioning physical space for each sensor, the sensor-to-target assignment problem reduces to that of determining which region the target falls in. This provides for a significant reduction of real time computational efforts for radar scheduling, but it also results in time periods that overwhelm individual sensor tracking capacities while under-utilizing other sensors. This results from intervals of time during which targets concentrate within a region at levels in excess of the time-averaged target density.

To account for the time variance in target densities, we reduce the amount of space D assigned to a specific sensor by including parameter γ in Equation (3.8), resulting in Equation (3.9). Location x in D is assigned to a partitioned region only if there exists a sensor i whose cost $\lambda_i \alpha_i \|x - p_i\|^4$ is less than the cost of assignment to all other sensors by at least γ. This results in an unassigned region in which targets may be tracked by any sensor.

$$R_i = \left\{ x \in D \quad | \quad \lambda_i \alpha_i \|x - p_i\|^4 \leq \lambda_j \alpha_j \|x - p_j\|^4 - \gamma \qquad \forall j \neq i \right\} \qquad (3.9)$$

Figure 3.4 displays the results of a uniform average target density with varying values of γ. As the magnitude of γ increases, the inequality becomes more difficult to satisfy and Equation (3.9) assigns less of the original space D to a specific sensor. As the range from the sensor network increases, the inequality becomes easier to satisfy as the magnitude of $\lambda_i \alpha_i \|x - p_i\|^4$ becomes much greater than γ. We present further results and analysis from this formulation in Section 4.2
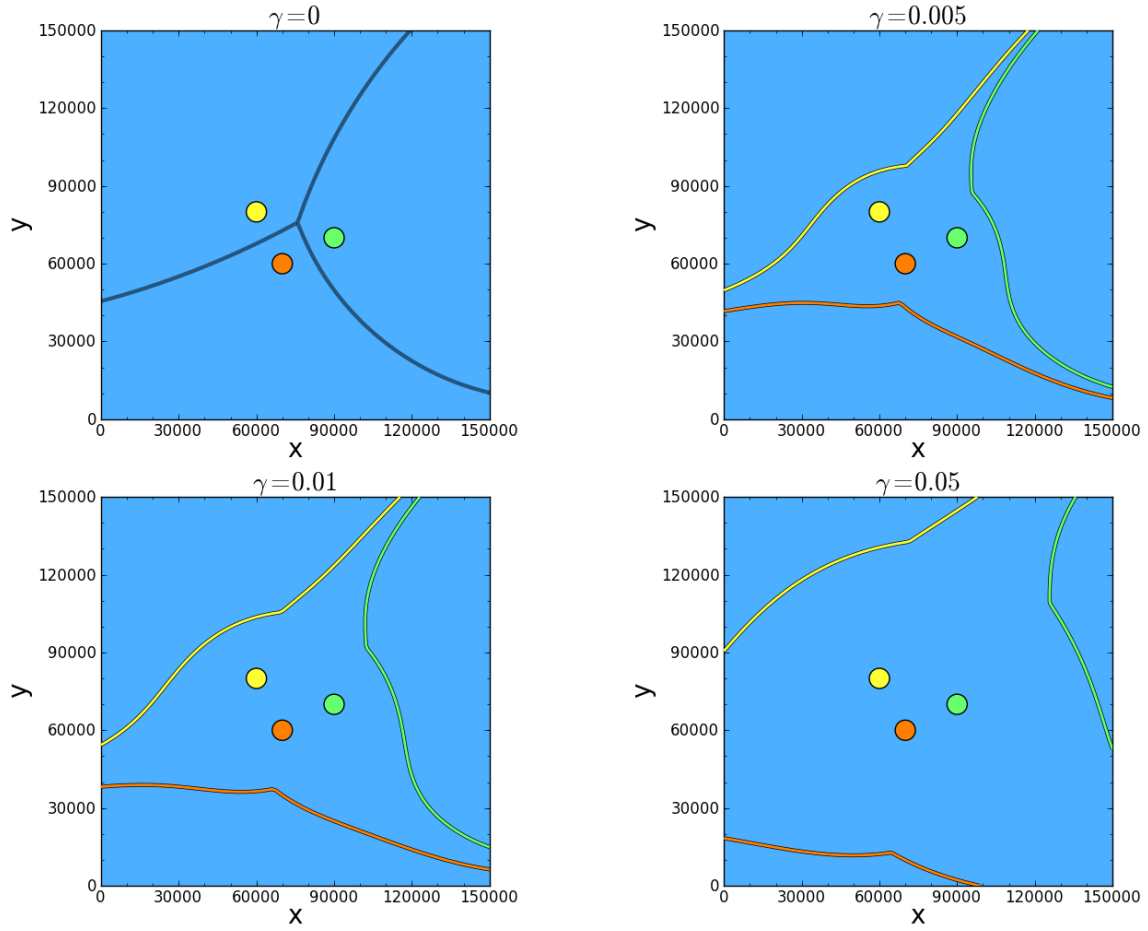
Figure 3.4: Effects of γ on the geographic partitioning results for three sensors in a uniform average target density.

3.3   Geographic Assignment with Handoff Penalties

In real world applications, transferring tracking responsibilities between sensors can consume additional radar resources. The uncertainty of a target's relative bearing and range, the dependence of RCS on the target and sensor geometry, and the potential for environmental interference can require additional effort by the newly assigned radar to establish the required track quality. To include these additional radar resource costs in a partitioning scheme, we introduce a model that incorporates handoff penalties.

3.3.1 Formulation

To account for handoffs, we discretize the formulation introduced in Section 3.1.1 and add a penalty for expected target tracks entering a region. To assess the penalty, we define specific directional target paths through the discretized space. The model penalizes a sensor if one of these paths enters its assigned region.

Without additional constraints, a target's assigned region may include the specified target paths to prevent a handoff penalty while ignoring the area between the path and the sensor. To prevent this, we enforce star convexity of the regions. For a discrete cell to be part of a sensor's assigned region, all of the cells between it and the sensor must also be in that region. The resultant mathematical formulation follows.

Index Use [~Cardinality]

$i \in I$ sensors [~3]

$j \in J$ targets [~30]

$k \in K$ geographic position (alias k') [~2500]

Sets

$(k, k', j) \in P$ k' is the discrete position that follows k along the path of target j

$(k, k', i) \in N$ k' is the neighboring discrete position closest to sensor i for position k

Given Data [Units]

$p_{i,k}$ energy cost to monitor discrete position k with sensor i [J]

ρ_k target density at geographic position k [targets/s]

α penalty for permitting handoffs [kW]

μ weighting factor to prioritize objectives [unitless]

Decision Variables [Units]

Z energy demands on maximally tasked sensor [J]

$X_{i,k}$ binary decision to assign position k to sensor i [binary]

$Y_{i,t,k}$ binary decision to gain target j with sensor i at position k [binary]

Formulation

$$\min_{X,Y,Z} Z + \mu \left(\sum_{i,k} \rho_k p_{i,k} X_{i,k} + \alpha \sum_{i,j,k} Y_{i,j,k} \right) \tag{3.10}$$

s.t.

$$Z \geq \sum_{k} \rho_k p_{i,k} X_{i,k} + \alpha \sum_{j,k} Y_{i,j,k} \qquad \forall i \tag{3.11}$$

$$Y_{i,j,k} \geq X_{i,k} - X_{i,k'} \qquad \forall i, \left(k, k', j \right) \in P \tag{3.12}$$

$$X_{i,k} - X_{i,k'} \leq 0 \qquad \forall i, \left(k, k', i \right) \in N \tag{3.13}$$

$$\sum_{i} X_{i,k} \geq 1 \qquad \forall k \tag{3.14}$$

$$Y_{i,j,k}, X_{i,k} \in \{0,1\} \qquad \forall i, j, k \tag{3.15}$$

3.3.2 Discussion

The objective function (3.10) minimizes the energy demands on the maximally tasked sensor and, subordinately, minimizes the overall energy demand. Constraints (3.11) ensure that Z tracks the maximum energy demanded of any sensor by bounding it by the energy demands of tracking and handoffs for each sensor. To enforce a handoff penalty, constraints (3.12) require $Y_{i,j,k}$ to be one if sensor i is assigned target j at position $X_{i,k}$ but was not assigned the previous location along the target's path, $X_{i,k'}$. Constraints (3.13) enforce star convexity of the assigned regions by ensuring that a discrete position k is not assigned to sensor i unless the path between i and k is also assigned to i. Constraints (3.14) ensure that each position $X_{i,k}$ is assigned to at least one sensor. Constraints (3.15) define the domains of the decision variables.

To demonstrate the results of this formulation, we project the target density function in Figure 3.2 onto two dimensions and discretize the results. Figure 3.5 displays the new expected target density within a 50 x 50 hexagonal grid. The three black lines represent the target paths for which the model assesses penalties if a handoff between sensors occurs.

Figure 3.6 presents the optimal results from this formulation when there is no handoff

penalty and when the penalty for handoffs is large. The results with no handoff penalty are similar to those we obtain with the continuous formulation of Section 3.1. When the penalty becomes adequately large, the cost of handoffs exceeds the costs of reassigning space to maintain track paths within a single sensor's region.
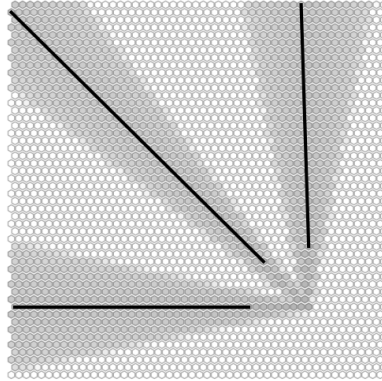

Figure 3.5: Two dimensional target density for one HVA with three directions of approach.
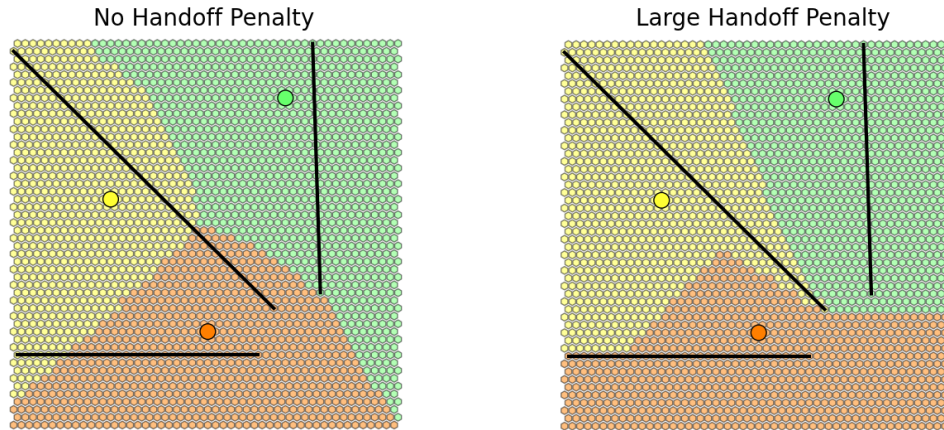

Figure 3.6: Results of geographic assignment with handoff penalties for the target density in Figure 3.5.

THIS PAGE INTENTIONALLY LEFT BLANK

CHAPTER 4:
RESULTS AND ANALYSIS

This chapter presents the results and insights from formulations presented in Chapters 2 and 3. We performed all computations on a Dell Precision T1650 PC with a 3.40 GHz Intel Core i7-3770 CPU and 16 GB of RAM. To solve the geographic assignment model of Section 3.1, we utilized MATLAB rev. R2012b. We implemented the other optimization models using the General Algebraic Modeling System (GAMS) rev. 236 and solved them with CPLEX 12.2.0.2. The details of specific problem instances, including approximate model sizes and computation times, are included in the following sections.

4.1 Maneuverable Targets

We investigate the impact of coordinated target maneuvers by using the model described in Section 2.3. For each scenario, the model contained approximately 250 decision variables, of which approximately 170 were discrete, and 200 constraints. Solution times were less than one second. To determine the "worst case" maneuver scheme, we considered 4096 possible maneuver combinations. The total model run time averaged two hours.

Figure 4.1 displays the schedules obtained for four scenarios. In each scenario, two sensors are tasked with tracking six targets. The sensors are capable of observing at most one target per time step. Upon commencement of tracking, the sensor network must observe each target at least once every three time steps. Thus, when tracking all six targets, the two sensors are operating at their maximum capacity. The sensors track each target for eight time steps. Following a target maneuver, three observations must occur within the next three time steps or a penalty is assessed. Maneuvers are not allowed after the fifth time step during which the target is tracked. This ensures the sensors have three time steps in which to perform the required observations. Each scenario varies only in the times at which tracking of the targets commence. In the first scenario, the sensors commence tracking all targets during the first time step. Target tracks commence at one, two and three second intervals in the second, third, and fourth scenario, respectively. For each scenario, we consider all feasible combinations of target maneuvers to determine which has the greatest impact on the radar tracking schedule.
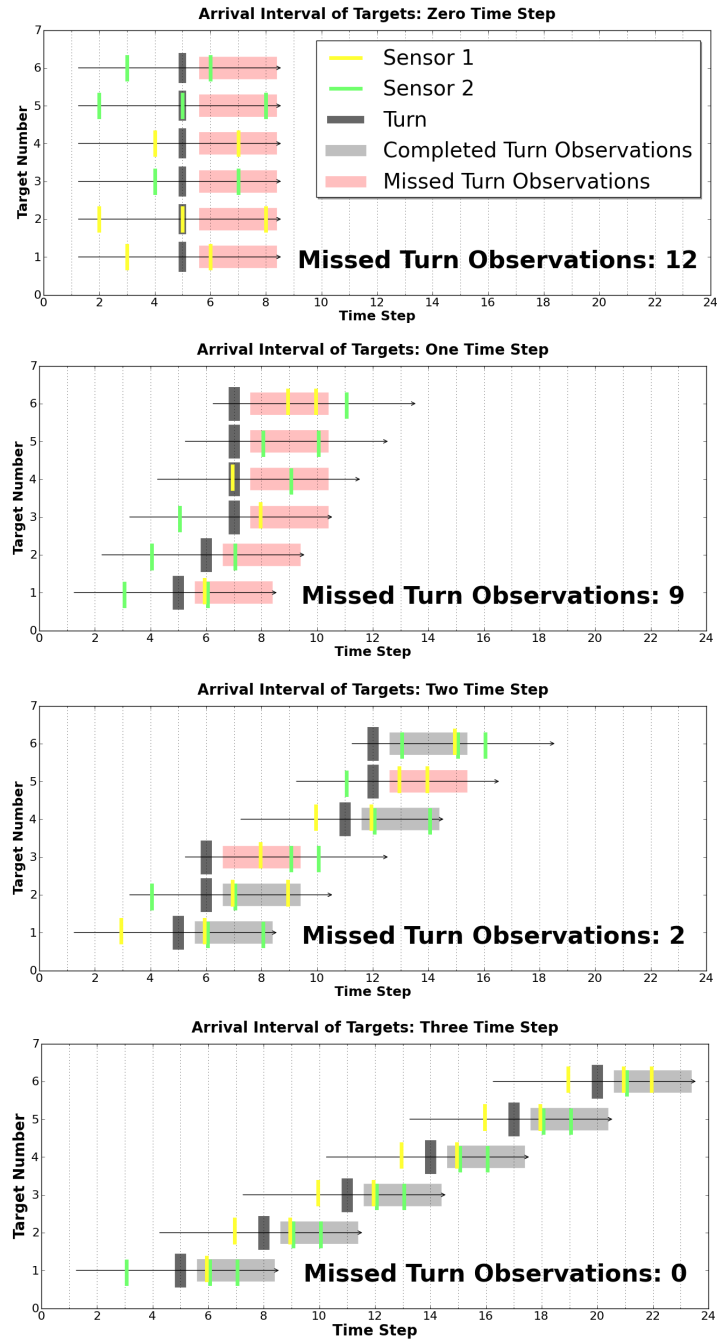
Figure 4.1: Optimal observation schedules with "worst case" maneuvers for four scenarios involving two sensors and six targets.

As demonstrated in the first scenario, the targets attempt to synchronize their maneuvers in order to maximize the demands for sensor assets in the following time steps. This results in a failure to perform sufficient observations on any target following the maneuver. As the interarrival time of target tracks increases, the targets become less effective at overwhelming sensor resources due to the inability to synchronize all of their maneuvers. By the fourth scenario, in which target tracks are offset at three second intervals, the targets are no longer able to coordinate their maneuvers so as to overwhelm the sensors.

These results suggest that adversarial targets could overwhelm a sensor network operating at or near its tracking capacity by effectively coordinating their operations. The impact on track quality of delayed observations, especially during this period of varying target speeds and directions, could result in the loss of a large number of hostile tracks. However, the effects diminish as targets lose the capability to effectively synchronize maneuvers.

4.2   Geographic Assignment

We now use the models from Sections 3.1 and 3.2 to analyze the performance of sensor-to-target assignments based on geographic partitioning. Each instance contained between 200,000 and 450,000 decision variables, of which 5,000 to 15,000 were discrete. The number of constraints ranged from 6,500 to 13,000. Typical solution times ranged from 10 seconds to 30 minutes per simulation. Solution times increased significantly when observation delays occurred.

Figure 4.2 and Figure 4.3 present the results of six scenarios involving three stationary sensors. Each scenario consists of a different number of targets, from 25 to 33, that have randomly assigned arrival and departure times within the 105 time steps considered. A sensor can perform at most one observation per time step, and the sensor network must observe each target at least once every 10 time steps or accept a delay penalty. Thus, a delay occurs any time the sensor network is monitoring more than 30 targets simultaneously. We conduct 120 simulations of target tracks for each scenario. For each simulation, we determine the "best case" schedule of observations by implementing the sensor-to-target assignment model of Section 2.2.
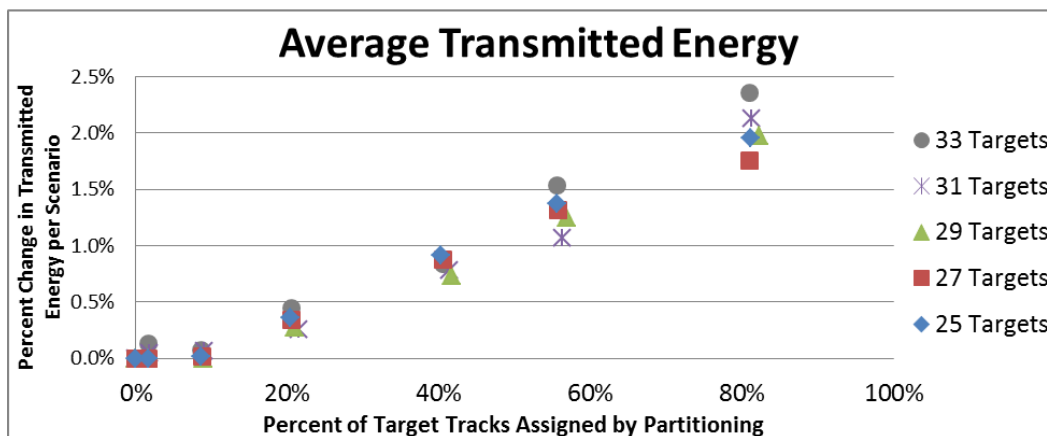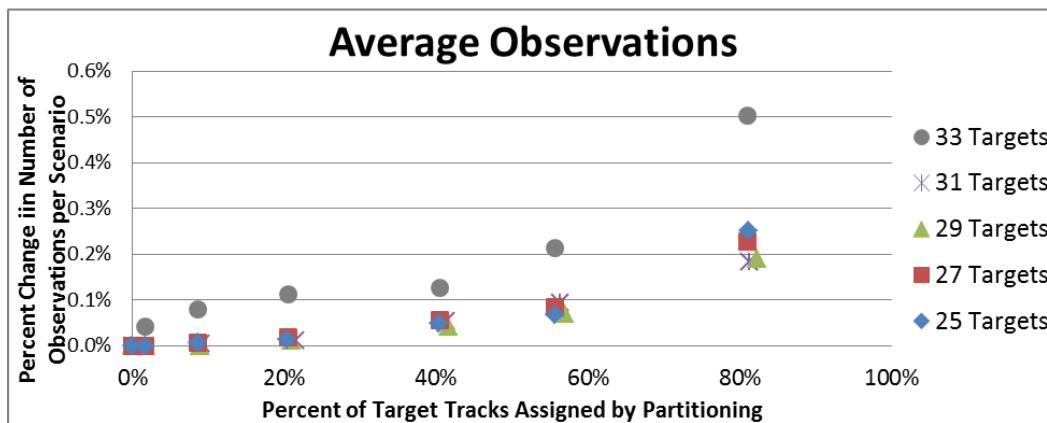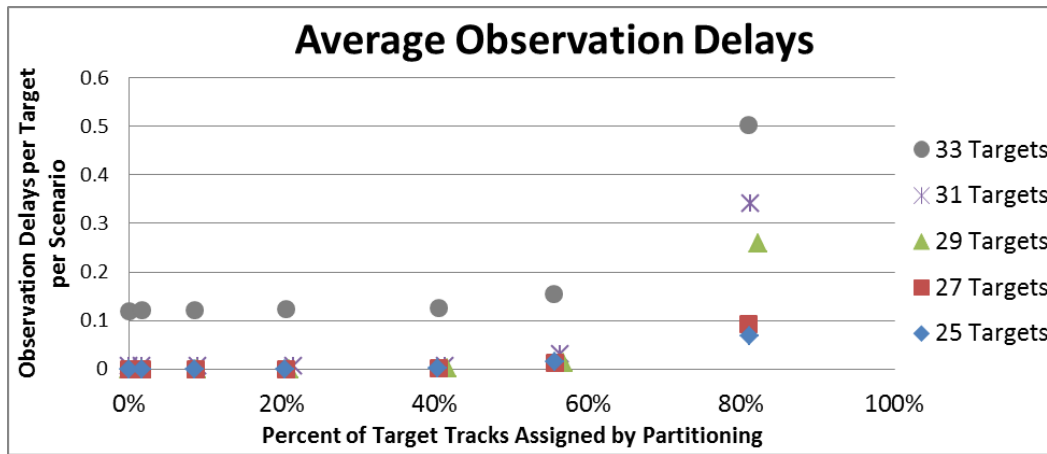
Figure 4.2: Average delays, observations, and transmitted energy for scenarios involving various target densities.
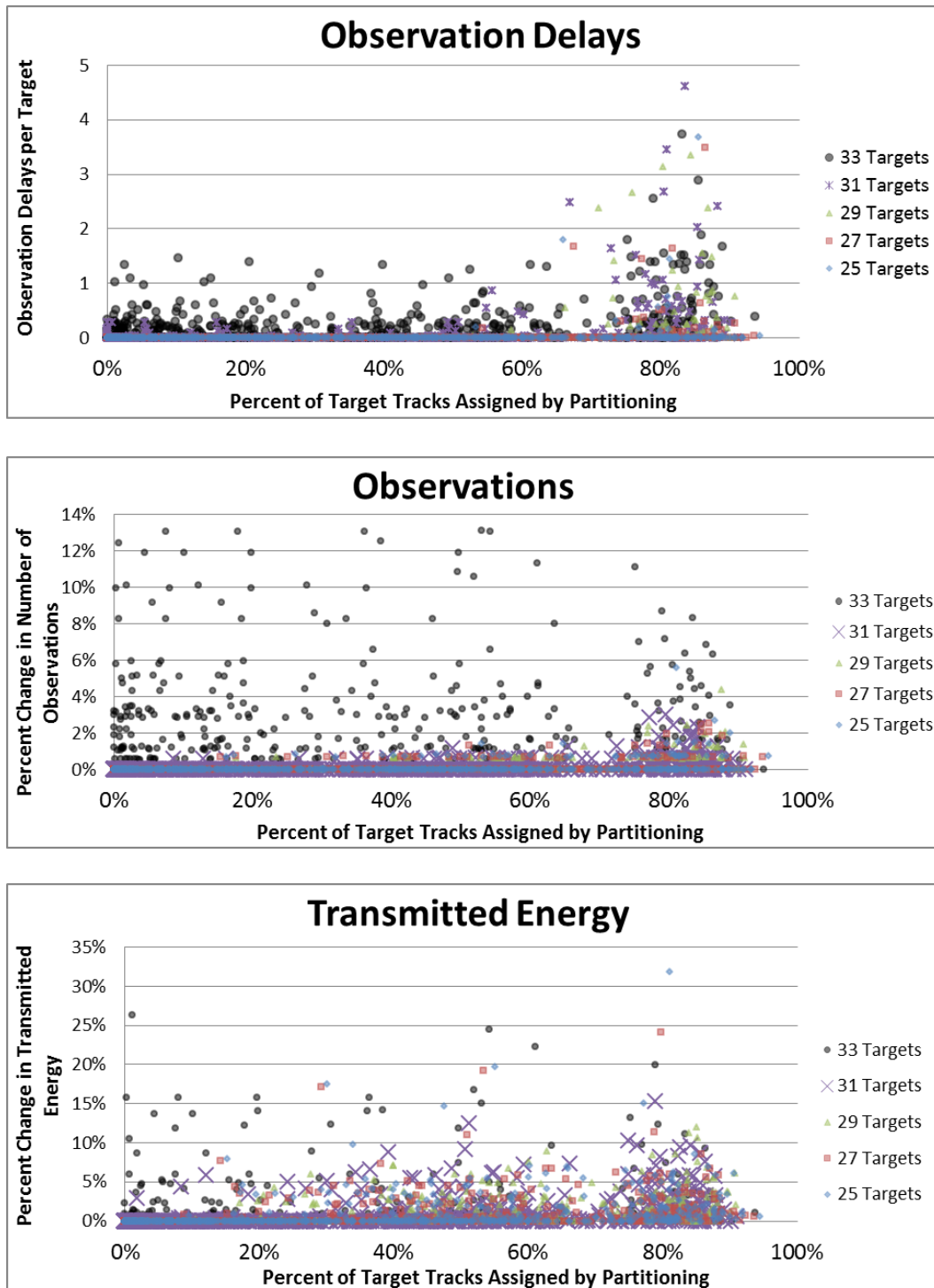
Figure 4.3: Delays, observations, and transmitted energy for each simulation of scenarios involving various target densities.

To investigate the effectiveness of the geographical partitioning approach developed in Section 3.2, we choose various values for γ and then solve for the "best case" schedule. The model restricts sensor assignments in the partitioned regions by only assigning waveforms from the designated sensor to the set of available observations $(i, j, t, k) \in P$. For each value of γ, we obtain the "best case" schedule for 120 simulations of each of the six scenarios.

Figure 4.2 displays the average number of delays, average number of observations required above optimal, and the average amount of energy required above optimal for each value of γ and number of targets. Figure 4.3 displays the number of delays, number of observations above optimal, and amount of energy above optimal required for each simulation. For all scenarios, the impact on the "best case" schedule appears to be relatively stable until the partitioning method assigns approximately 40 percent of the target tracks to sensors. After this point, the number of delays increases significantly as targets overwhelm the sensors' tracking capacities when they concentrate within a single sensor's region of responsibility.

We perform similar analyses to investigate the impact of different sensor network sizes and geometries. The sensor capabilities remain the same as in the previous scenarios. We establish three new scenarios for comparison: three sensors and 30 targets, four sensors and 40 targets, and five sensors and 50 targets. The number of sensors and targets maintain a constant ratio across scenarios; this allows us to observe the effect of preassigning sensors to targets on networks operating at their tracking capacity. Figure 4.4 displays the three sensor networks, including "best case" results from 60 simulations with and without partitioning. For six values of γ, we obtain the "best case" schedule for 60 simulations of each of the three scenarios.

Figure 4.5 and Figure 4.6 display the resulting delays, the number of observations, and the energy emitted. Again, the impact appears to be relatively stable until partitioning accounts for approximately 40 percent of sensor-to-target assignments. However, the relative impact of partitioning on the larger networks appear to be greater than that observed with three sensors. Worth noting are the average number of observations performed by the four- and five-sensor networks when the partitioning accounts for approximately 80 percent of target track assignments. Rather than continue the trend of requiring additional observations as more of the operating space is partitioned, these scenarios utilize less observations on average than the scenarios where partitioning accounts for approximately 50 to 60 percent of the

target assignments. This is due to the significant increase in delays for both networks when the partitioning method preassigns too many targets and overwhelms individual sensors.

These preliminary results suggest that assigning a portion of targets to sensors based on their geographic location may provide an efficient heuristic approach for reducing the number of real time sensor-to-target assignments that other, more sophisticated algorithms must perform.
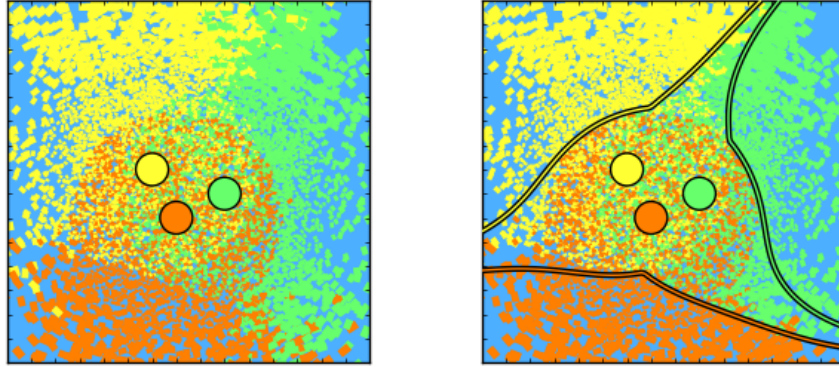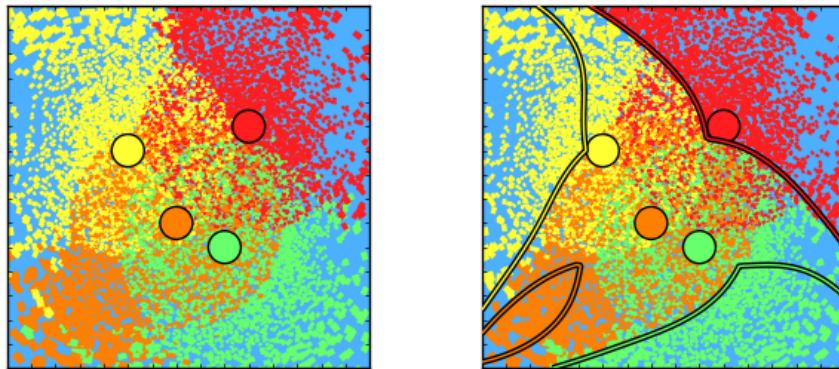
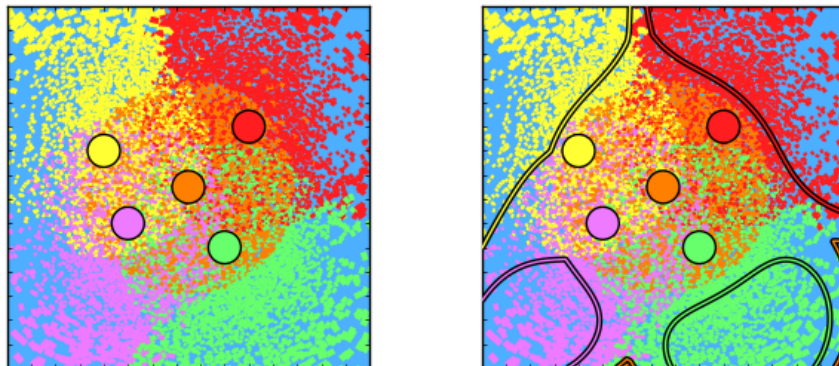Figure 4.4: Observations from optimal schedules, with and without geographic partitioning, for 60 simulations of scenarios involving three, four, and five sensors.
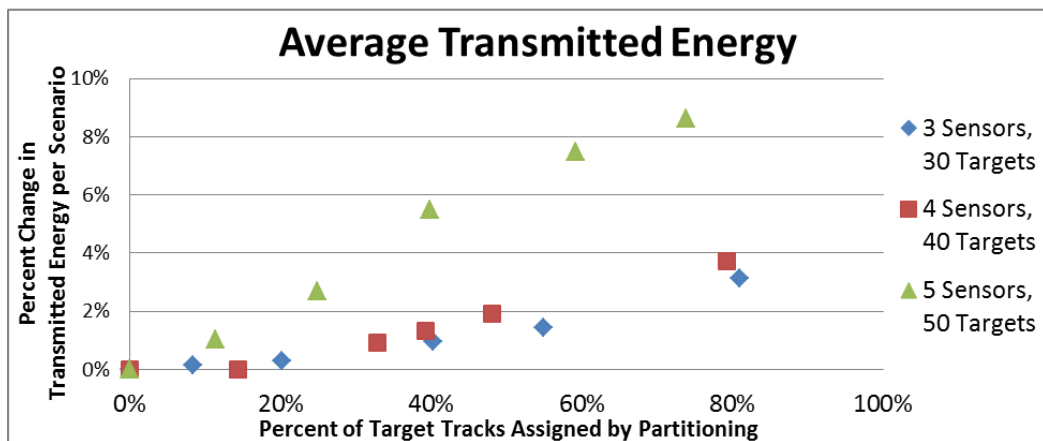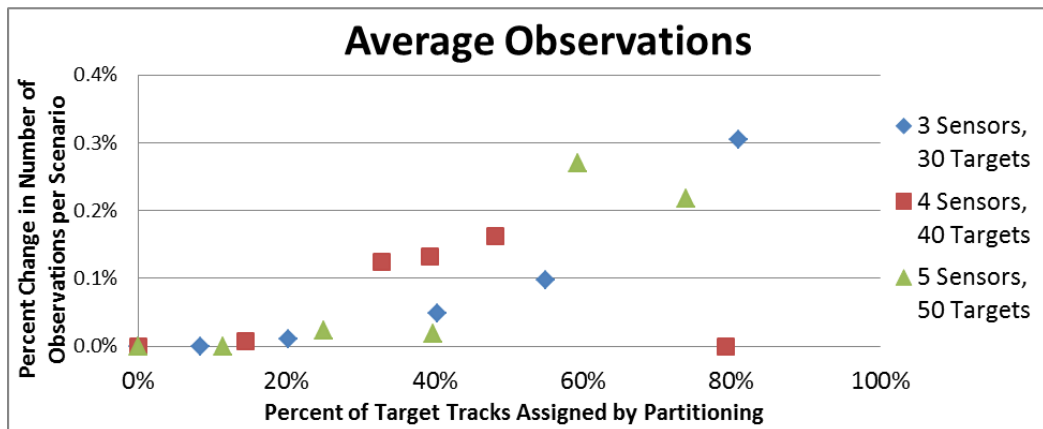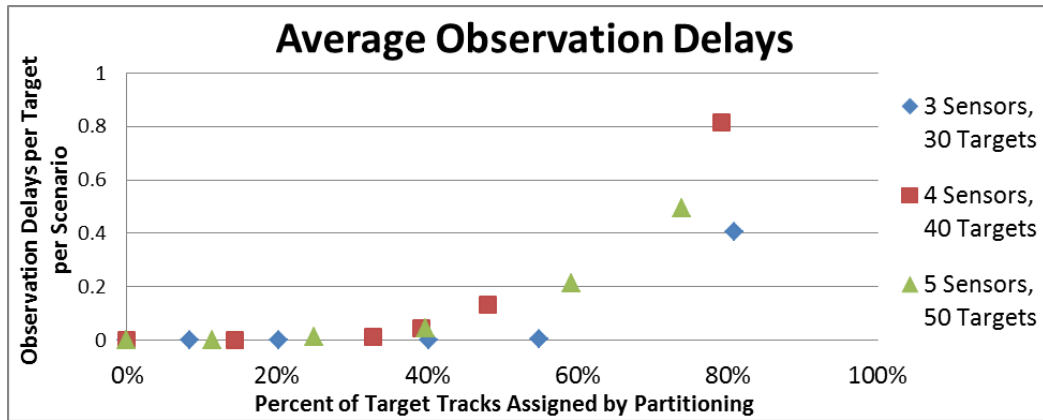
Figure 4.5: Average delays, observations, and transmitted energy for scenarios involving three, four, and five sensors.
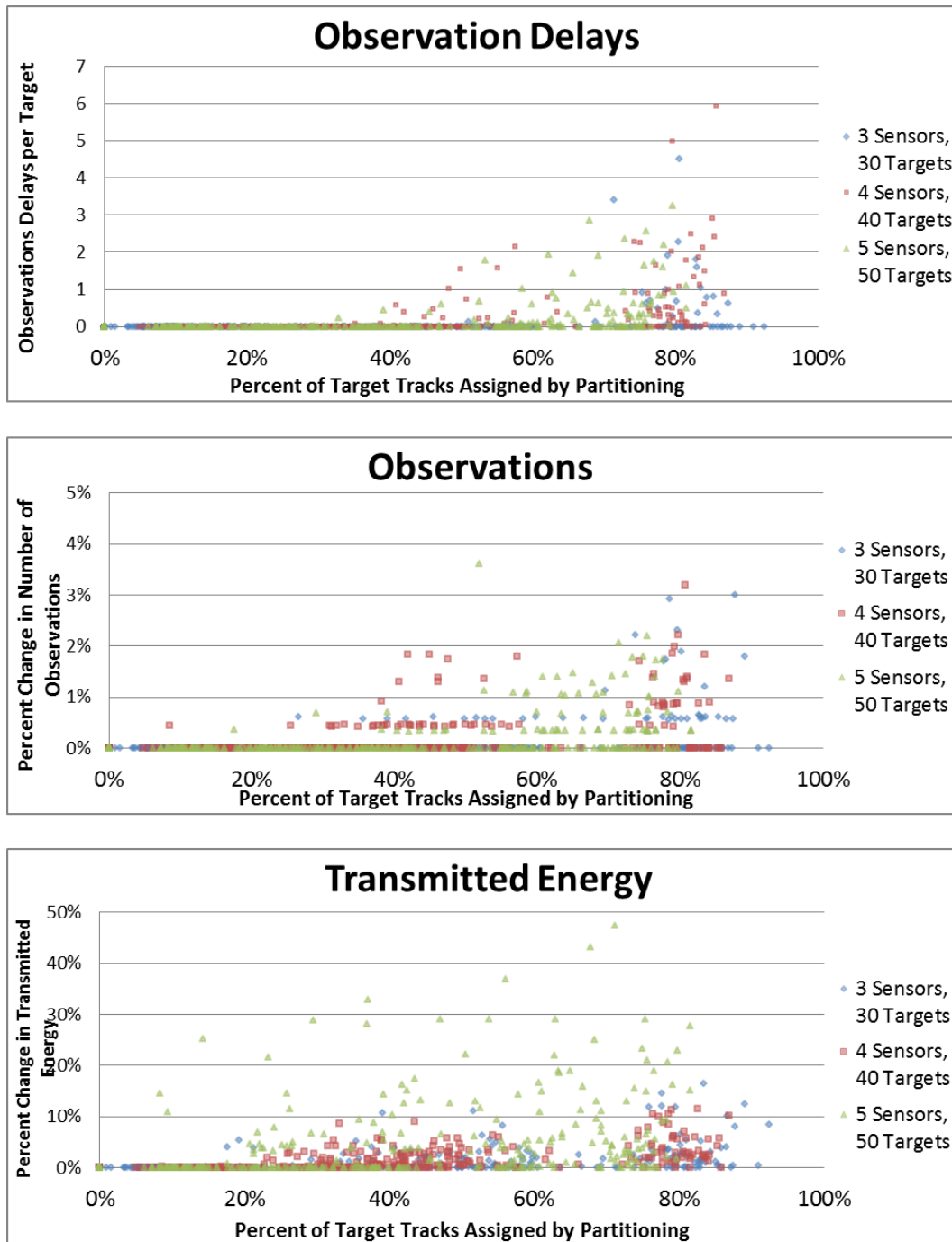
Figure 4.6: Delays, observations, and transmitted energy for each simulation of scenarios involving three, four, and five sensors.

4.3   Geographic Assignment with Handoff Penalties

To account for resource costs resulting from the transfer of tracking responsibility between sensors, we utilize the formulation presented in Section 3.3. We consider the scenario where targets approach a single HVA from three directions. Figure 4.7 (a reproduction of Figure 3.5) represents the target density obtained by projecting Figure 3.2 onto two dimensions and discretizing the results into a 50 x 50 hexagonal grid. The three black lines represent the target paths for which penalties are assessed if a handoff between sensors occurs. During a target handoff, the sensor receiving responsibility for the target must perform extra work to establish the required track quality. Thus, the model only assesses a penalty on the sensor gaining the target.
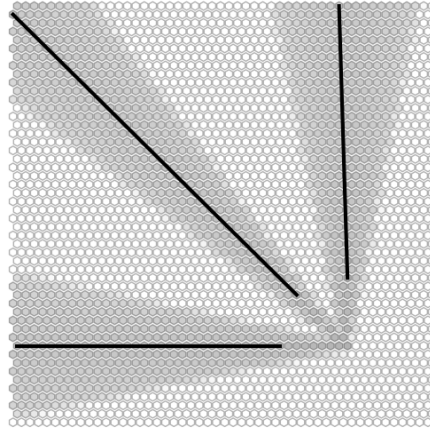
Figure 4.7: Two dimensional target density for one HVA with three directions of approach.

To determine the potential effects of target handoffs on optimal geographic partitioning, we vary the handoff penalty α in 1 kW increments from 0 to 5 kW. Each instance contained approximately 30,000 decision variables, of which all but five were discrete, and 10,300 constraints. Typical solution times were less than two seconds. Figure 4.8 and Table 4.1 display the results of this analysis.
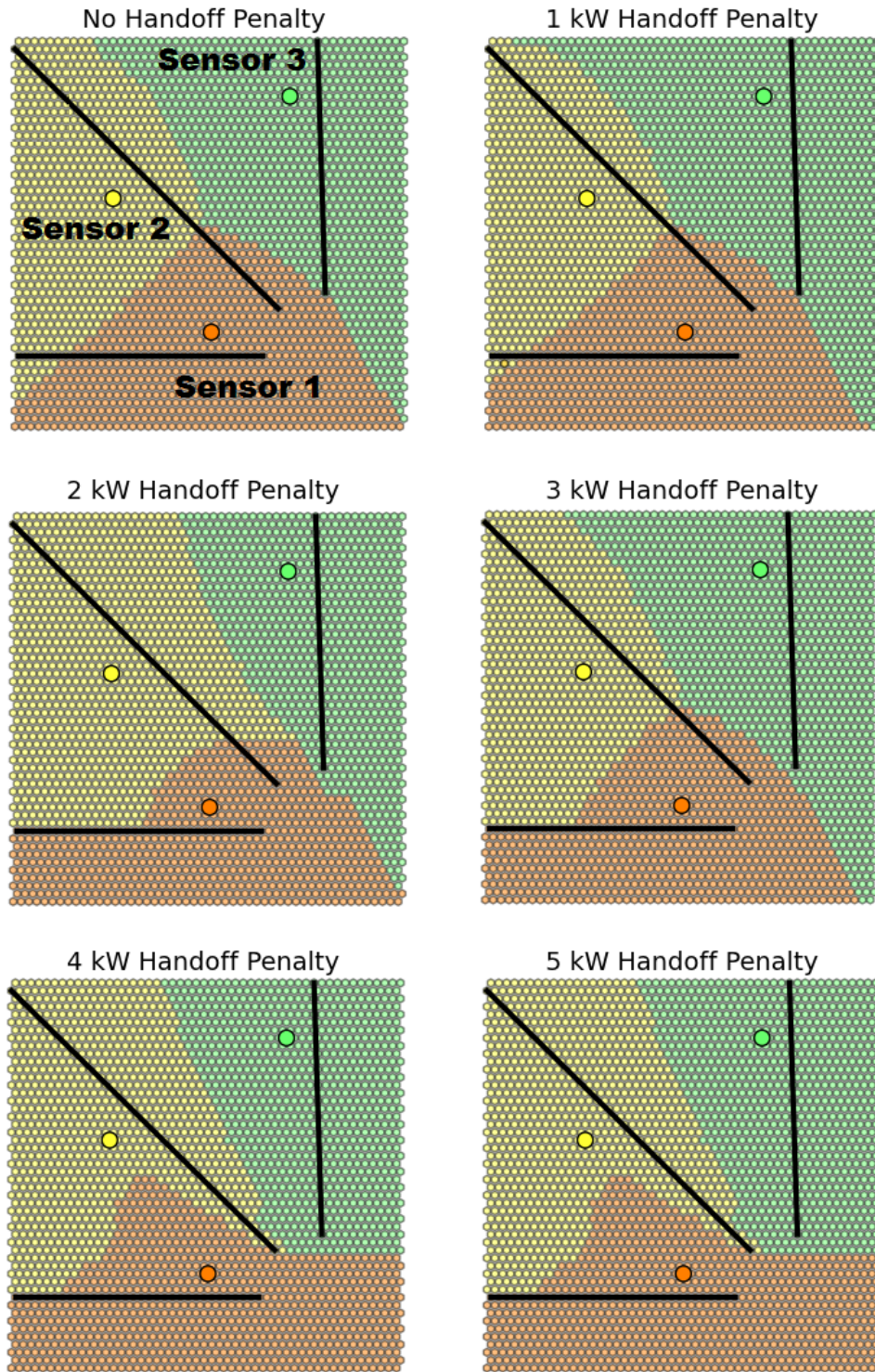
Figure 4.8: Results of geographic assignment with various handoff penalties for the target density in Figure 4.7.

Handoff Penalty (α) kW	Individual Sensor Sensor Requirements kW	Total Network Sensor Requirements kW	Number of Handoffs
0	3.97	11.91	2
1	4.97	14.91	2
2	5.53	16.59	1
3	5.67	17.01	1
4	5.79	17.37	0
5	5.79	17.37	0

Table 4.1: Sensor energy demands and number of handoffs for geographic assignments with various handoff penalties for the target density in Figure 4.7.

When there is no handoff penalty ($\alpha = 0$kW), the resulting partition matches that obtained from the continuous geographic partitioning formulation. In this scenario, even without handoff penalties, one of the target paths remains completely within the region assigned to Sensor 3 and no handoff occurs. As α increases to 1kW, the other two target paths continue to transit between regions, but the partitioned regions adapt to the increased demands on the receiving sensor, Sensor 1. In order to minimize the maximum workload on any sensor, Sensor 1 shifts some of its region to other sensors, such as the lower right corner of the operating space, to equalize the increased burden across the sensor network. This transfer of regions between sensors costs the system additional resources since the range between the regions and their assigned sensors increases. Thus, while the total handoff penalty in this case is 2 kW, the total network radar resource requirement rises from 11.91 to 14.91 kW, a 3 kW increase.

When the handoff penalty exceeds approximately 1.5 kW, the costs of accepting two handoff penalties exceeds the costs of reassigning regions among sensors and one of the target paths is completely absorbed by Sensor 1. As the handoff penalty increases to 2 and 3 kW, regions shift from Sensor 1 to equalize resource demands between sensors.

Around 4 kW, the handoff penalty becomes so high that the sensor network does not accept any handoffs. In this scenario, each of the sensors maintains one of the target paths from

start to finish. Any additional increase in handoff penalty has no effect on the partitioned regions since no handoffs occur.

While the partitioned regions adapt to any changes in handoff penalties, a reduction in the number of handoffs requires these penalties to be a large percentage of the network's radar demands. The system removed a handoff only when the penalties exceeded approximately 25 percent of total demands on the sensor network's resources. To remove both handoffs, the total resource requirements for the sensor network increases by 45 percent. Thus, for the scenario considered, the amount of resources demanded to execute a handoff between sensors must be relatively high compared to other tracking requirements before it becomes advantageous to significantly alter the partitioned regions to limit handoffs. Analysis of additional scenarios may yield insights into the generality of these results.

CHAPTER 5:
CONCLUSION

The coordination of networked sensors is critical to obtaining superior functionality and battle space awareness. By synchronizing tracking efforts in a cluttered target environment, individual platforms can redirect resources to unit-specific operations or other radar functions. This thesis develops several models to analyze target assignments in a multiple-sensor network.

We develop an optimization model that uses full target information to provide a "best case" assessment of the ability of a given set of radar platforms to track a collection of targets. A modified version of this model determines the impact on these results if targets coordinate their maneuvers in an attempt to exceed the resource capacity of the sensor network. Results suggest that synchronized maneuvers may produce situations whose sensor resource demands exceed network capabilities. This could result in reduced track quality leading to higher track loss rates.

We also consider the more realistic scenario in which the planner's knowledge is imperfect and describe approaches for allocating sensor assets to targets based on geographic location. The first method extends an existing two-dimensional geographic allocation approach to three dimensions. By adjusting how much of the operating space the model assigns to a specific sensor, we develop a heuristic approach for preassigning sensors to targets that has the potential to reduce the computational demands of more sophisticated assignment algorithms. In the scenarios examined, the heuristic can perform approximately 40 percent of sensor-to-target assignments with a limited impact on the "best case" assessment results. This could lead to significant reductions in real time computations and data transfer rates required by sensor-to-target assignment algorithms.

Finally, we investigate the impact of transferring target tracking requirements between sensors by developing a model that permits the inclusion of handoff penalties. In order to do so, we modify the previously mentioned partitioning model by discretizing the operating space and defining target paths through this space. Any sensor that gains part of the path

after it begins is assessed a handoff penalty to account for the additional resources required when transferring a target between sensors. For the scenario considered, we find that significant modifications to the sensors' regional assignments only occur if the resource demands for target handoffs account for more than 25 percent of the total demand.

5.1 Further Research Topics

Several avenues of research exist to continue investigating this problem. A number of interesting extensions arise simply by relaxing the assumption that every observation results in the same information gain.

Radar returns and return-to-track correlation are not without error. An investigation into the effects of false negative and false positive observations along with the potential for mis-correlation could lead to a greater appreciation of actual resource requirements for a given scenario. A possible approach could include utilization of a dynamic programming model to analyze the potential impacts of choosing different waveforms or delaying observations.

Environmental factors also have a significant impact on radar performance. Future analysis could explore this effect by adapting some of the models introduced in this thesis to allow for the emplacement of physical obstacles in the operating space, such as land or weather events. Additionally, target aspect can affect the RCS observed by different sensors. Expansion of the models presented in this thesis to allow for unique target RCSs for each sensor is another possible research topic.

In addition to external factors, design limitations also impact an MFR's performance. MFR arrays are not capable of transmitting in all directions. As the angle between the direction of the radar beam and the array's broadside increases, the emitted power becomes more diffuse and less effective at tracking. To overcome these limitations, the AN/SPY-1 MFR uses four arrays to provide 360 degree coverage. Future research could investigate how a sensor's limited coverage angle affects the decision of how to schedule target observations.

By allowing for varying levels of information gain, the possibility arises that the assignment of multiple sensors to a single target may result in superior track quality. This thesis does not investigate this possibility and the models presented provide a single sensor-to-target assignment. Development of a model that allows for multiple sensors-to-target assignment

during each time step would more closely represent the problem faced by networked MFRs.

While relaxing our assumptions concerning information gain presents numerous challenges worth exploring, future research could also focus on the heuristic approach presented to allocate targets to sensors geographically. The proposed benefit of this method is to reduce the number of sensor-to-target assignment decisions that must be made in real time. Future analysis could determine the actual reduction in real time computations provided by this heuristic when implemented with existing assignment models, such as those presented in the literature review of Section 1.2.

Future research could also compare the results to other geographic assignment models. It is possible that a simpler approach leads to similar or more effective sensor-to-target assignment. Additionally, the geometry of the sensor network might impact the effectiveness of the heuristic. If there are interior sensors, such as in a layered defensive position, only the exterior sensors have an advantage when observing distant targets. Limiting geographic assignment to a subset of available sensors may result in superior performance of the heuristic.

Several of the simulated scenarios result in periods of time during which targets overwhelm a single sensor's tracking capability. To account for this, future research could focus on the development of a contingency algorithm that allows for the reassignment of targets that oversaturate a region. The algorithm would need to determine which targets become available for other sensors to observe, when the targets become available, and how to transfer the responsibility for tracking between sensors.

The challenges of protecting HVAs continue to grow with the rapid proliferation of aerial assets. Coordination of available defensive capabilities is critical to defeating this threat. This thesis provides several models for investigating the benefits of networked MFRs. As long as an effective air defense remains elusive, research of this topic will remain paramount.

THIS PAGE INTENTIONALLY LEFT BLANK

Appendix: Proof of Duality and Optimality for Geographic Partitioning

This appendix presents the derivation of the dual problem (Section 3.1.3) for the linear relaxation of the geographic assignment model presented in Section 3.1 and provides the proof of optimality for the partition presented as Equation (3.8). This appendix parallels work presented by Carlsson (2012) with modifications of the formulations to account for three dimensions and the specific parameters and nomenclature introduced in this thesis.

Derivation of Dual to Geographic Assignment Model

This derivation is a simple proof "sketch" for obtaining the dual formulation by discretizing the original problem. For a more rigorous mathematical proof, refer to Appendix A of (Carlsson, 2012).

The geographic partition model considered is provided as Equations (1) and (2).

$$\min_{R_1,\ldots,R_n} \max_i \iiint_{R_i} \alpha_i \rho(x) \|x - p_i\|^4 \, dV \tag{1}$$

s.t.

$$\bigcup_{i=1}^{n} R_i = D \tag{2}$$

This problem is reformulated as an infinite-dimensional integer program in Equations 3–6.

$$\min_{I_1(\cdot),\ldots,I_n(\cdot)} t \tag{3}$$

s.t.

$$t \geq \iiint_D I_i(x)\alpha_i\rho(x)\|x - p_i\|^4 \, dV \qquad \forall i \quad (4)$$

$$\sum_{i=1}^{n} I_i(x) = 1 \qquad \forall x \in D \quad (5)$$

$$I_i(x) \in \{0,1\} \qquad \forall i, x \in D \quad (6)$$

where $I_i(x)$ is 1 if x is assigned to facility i and 0 otherwise.

Without loss of generality, we can relax the equality constraint of Equation (5). Relaxation of the integer constraint (Equation (6)) results in the following infinite-dimensional linear program (Equations 7–10).

$$\min_{I_1(\cdot),\ldots,I_n(\cdot)} t \qquad (7)$$

s.t.

$$t \geq \iiint_D \alpha_i\rho(x)\|x - p_i\|^4 \, dV \qquad \forall i \quad (8)$$

$$\sum_{i=1}^{n} I_i(x) \geq 1 \qquad \forall x \in D \quad (9)$$

$$I_i(x) \geq 0 \qquad \forall i, x \in D \quad (10)$$

Discretization of the operating space into grid cells indexed by k admits the following formulation (Equations 11–14).

$$\min_{x,t} t \qquad (11)$$

s.t.

$$t \geq \varepsilon \sum_{k} c_{i,k}x_{i,k} \qquad \forall i \quad (12)$$

$$\sum_{i=1}^{n} x_{i,k} \geq 1 \qquad\qquad\qquad \forall k \quad (13)$$

$$x_{i,k} \geq 0 \qquad\qquad\qquad \forall i,k \quad (14)$$

where ε is the volume of each grid cell, $c_{i,k}$ is the value of $\alpha_i \rho(x) \|x - p_i\|^4$ evaluated at the center of grid cell k, and $x_{i,k}$ represents the fraction of grid cell k assigned to sensor i. The dual of this formulation is presented as Equations 15–18.

$$\max_{q,r} \sum_{k} q_k \qquad\qquad\qquad (15)$$

s.t.

$$q_k \leq \varepsilon c_{i,k} r_i \qquad\qquad\qquad \forall i,k \quad (16)$$

$$\sum_{i=1}^{n} r_i \leq 1 \qquad\qquad\qquad (17)$$

$$r_i, q_k \geq 0 \qquad\qquad\qquad \forall i,k \quad (18)$$

By introducing the variable $q_k' := q_k/\varepsilon$, we can rewrite the dual as Equations 19–22.

$$\max_{q',r} \varepsilon \sum_{k} q_k' \qquad\qquad\qquad (19)$$

s.t.

$$q_k' \leq c_{i,k} r_i \qquad\qquad\qquad \forall i,k \quad (20)$$

$$\sum_{i=1}^{n} r_i \leq 1 \qquad\qquad\qquad (21)$$

$$r_i, q_k' \geq 0 \qquad\qquad\qquad \forall i,k \quad (22)$$

By reducing ε so that the grid cells become infinitesimal, the dual formulation can be rewritten as Equations 23–26.

$$\max_{\lambda,\sigma} \iiint_D \sigma(x)\mathrm{d}V \qquad (23)$$

s.t.

$$\sigma(x) \leq \lambda_i \alpha_i \rho(x)\|x - p_i\|^4 \qquad \forall x, i \ (24)$$

$$\sum_i \lambda_i \leq 1 \qquad (25)$$

$$\lambda_i \geq 0 \qquad \forall i \ (26)$$

This is exactly the dual formulation presented in Section 3.1.3.

Proof of Optimality of Geographic Partitioning Assignment

This section provides the proof that Equation (3.9) (reproduced as Equation (27)) results in the optimal partitioning of the operating space for the model presented in Section 3.1.1.

$$R_i = \left\{ x \in D \quad | \quad \lambda_i \alpha_i \|x - p_i\|^4 \leq \lambda_j \alpha_j \|x - p_j\|^4 - \gamma \qquad \forall j \neq i \right\} \qquad (27)$$

Theorem. Let λ^* be the weight vector obtained by solving the dual problem (Equations 23–26). Then setting

$$I_i^*(x) = \begin{cases} 1 & \text{if } x \in R_i^* \\ 0 & \text{otherwise} \end{cases},$$

with $\{R_1^*, \ldots, R_n^*\} = \mathfrak{R}(D, I, \lambda^*)$, is an optimal partition of D with respect to the infinite-dimensional integer programming formulation of the primal (Equations 3–6).

Proof. For any nonzero objective value of the dual (Equation (23)), Equation (24) requires $\lambda_i > 0$ for all i. For reasonable values (i.e., positive) of α_i and $\rho(x)$, any feasible combination of $\lambda_i > 0$ for all i results in a positive objective value. Therefore the optimal objective value for the dual must be positive and $\lambda_i^* > 0$ for all i. It follows from complementary slackness that Equation (4) is binding for all i ($t^* = \iiint_D I_i(x)^* \alpha_i \rho(x)\|x - p_i\|^4 \mathrm{d}V$ for all

60

i). Thus, $\iiint\limits_{R_i^*} \alpha_i \rho(x) \|x - p_i\|^4 \, dV = \iiint\limits_{R_1^*} \alpha_1 \rho(x) \|x - p_1\|^4 \, dV$ for all i. Plugging λ^* and the $\sigma^*(x)$ into the dual yields

$$
\begin{aligned}
\iiint\limits_{D} \sigma^*(x) \, dV &= \iiint\limits_{D} \min_i \lambda_i^* \alpha_i \rho(x) \|x - p_i\|^4 \, dV \\
&= \sum_{i=1}^{n} \lambda_i^* \iiint\limits_{R_i^*} \alpha_i \rho(x) \|x - p_i\|^4 \, dV \\
&= \sum_{i=1}^{n} \lambda_i^* \iiint\limits_{R_1^*} \alpha_1 \rho(x) \|x - p_1\|^4 \, dV \\
&= \iiint\limits_{R_1^*} \alpha_1 \rho(x) \|x - p_1\|^4 \, dV \qquad \text{(Because } \sum_{i=1}^{n} \lambda_i^* = 1 \text{)} \\
&= \iiint\limits_{D} I_i^*(x) \alpha_1 \rho(x) \|x - p_1\|^4 \, dV
\end{aligned}
$$

which completes the proof.

THIS PAGE INTENTIONALLY LEFT BLANK

References

Bar-Shalom, Y., & Li, X. R. (1995). *Multitarget-multisensor tracking: Principles and techniques*. Storrs, CT: YBS Publishing.

Billiter, D. R. (1989). *Multifunction array radar*. Norwood, MA: Artech House.

Blackman, S. S. (1986). *Multiple-target tracking with radar applications*. Norwood, MA: Artech House.

Blair, W., & Watson, G. (1996). *Benchmark problem for radar resource allocation and tracking maneuvering targets in the presence of ECM* (NSWCDD/TR-96/10). Dahlgren VA: Naval Surface Warfare Center Dahlgren Division. Retrieved from `http://www.dtic.mil/cgi-bin/ GetTRDoc?Location=U2&doc=GetTRDoc.pdf&AD=ADA286909`

Bogler, P. L. (1990). *Radar principles with applications to tracking systems*. New York: Wiley.

Camazine, S., Deneubourg, J., Franks, N., Sneyd, J., Theraulaz, G., & Bonabeau, E. (2001). *Self-organization in biological systems*. Princeton, NJ: Princeton University Press.

Carlsson, J. G. (2012). Dividing a territory among several vehicles. *INFORMS Journal on Computing*, *24*, 565–577. doi: 10.1287/ijoc.1110.0479

Dormon, F., Leung, V., Nicholson, D., Siva, E., & Williams, M. (2005, May). Information-based decision making over a data fusion network. *Proceedings SPIE*, *5809*, 100–110. doi: 10.1117/12.604825

Eberhart, R., & Kennedy, J. (1995). A new optimizer using particle swarm theory. *Proceedings of the Sixth International Symposium on Micro Machine and Human Science* (pp. 39–43). doi: 10.1109/MHS.1995.494215

Hura, M., McLeod, G., Schneider, J., Gonzales, D., Norton, D. M., Jacobs, J., . . . Jamison, L. (2000). *Tactical data links* (Monograph Report No. 1235). Santa Monica, CA: RAND Corporation. Retrieved from `http://www.rand.org/pubs/monograph_reports/MR1235.html`

Jane's Information Group. (2011). Link 16. In *Jane's electronic mission aircraft*. Alexandria, VA: Author. Retrieved from `https://janes.ihs.com.libproxy.nps.edu/CustomPages/Janes/ DisplayPage.aspx?DocType=Reference&ItemId=+++1309827&Pubabbrev=JEMA`

Jane's Information Group. (2012). Aegis; DANCS; COMBATSS-21. In *Jane's naval weapon systems*. Alexandria, VA: Author. Retrieved from `https://janes.ihs.com.libproxy.nps.edu/CustomPages/Janes/DisplayPage.aspx?DocType=Reference&ItemId=+++1316172&Pubabbrev=JNWS`

Johns Hopkins Applied Physics Lab. (1995). The cooperative engagement capability. *Johns Hopkins APL Technical Digest*, *16*, 377–396. Retrieved from `http://techdigest.jhuapl.edu/td/td1604/APLteam.pdf`

Lambert, H. C., & Sinno, D. (2011). Bioinspired resource management for multiple-sensor target tracking systems. *Proceedings of IEEE Sensors 2011 Conference* (pp. 1189–1192). doi: 10.1109/ICSENS.2011.6126904

Lockheed Martin. (2009). *SPY-1 family of radars: Battle-proven naval radar performance* [Brochure]. Retrieved from `http://www.scribd.com/doc/69977421/SPY-1-Family-Brochure-6-Pager`

McIntyre, G. A., & Hintz, K. J. (1996, June). Information theoretic approach to sensor scheduling. *Proceedings SPIE*, *2755*, 304–312. doi: 10.1117/12.243172

Nash, J. M. (1977). Optimal allocation of tracking resources. *Proceedings of the 1977 IEEE Conference on Decision and Control including the 16th Symposium on Adaptive Processes and A Special Symposium on Fuzzy Set Theory and Applications* (pp. 1177–1180). doi: 10.1109/CDC.1977.271748

National Research Council. (2008). *Evaluation of the multifunction phased array radar planning process*. Washington, DC: The National Academies Press. Retrieved from `http://www.nap.edu/openbook.php?record_id=12438`

Sabatini, S., & Tarantino, M. (1994). *Multifunction array radar: System design and analysis*. Norwood, MA: Artech House.

Schmaedeke, W. W. (1993, September). Information-based sensor management. *Proceedings SPIE*, *1955*, 156–164. doi: 10.1117/12.154970

Schmaedeke, W. W., & Kastella, K. D. (1998, September). Information-based sensor management and IMMKF. *Proceedings SPIE*, *3373*, 390–401. doi: 10.1117/12.324633

U.S. Army Air Land Sea Application Center. (2000). *Introduction to tactical digital information link j and quick reference guide (TADIL J)* (Field Manual 6-24.8). Langley, VA: Army Training and Doctrine Command. Retrieved from `http://www.dtic.mil/cgi-bin/GetTRDoc?Location=U2&doc=GetTRDoc.pdf&AD=ADA404334`

U.S. Navy. (2013). *United States Navy fact file: Aegis Weapon System.* Retrieved from `http://www.navy.mil/navydata/fact_display.asp?cid=2100&tid=200&ct=2`

U.S. Navy Naval Air Systems Command Director of Electronic Warfare/Combat Systems. (2012). *Electronic warfare and radar systems engineering handbook* (NAWCWD TP 8347). Point Mugu, CA: Naval Air Warfare Center Weapons Division. Retrieved from `http://www.dtic.mil/get-tr-doc/` `pdf?Location=U2&doc=GetTRDoc.pdf&AD=ADA566236`

Veeramachaneni, K., & Osadciw, L. A. (2006). Multiple sectors, multi function, multi radar dwell time management using particle swarm optimization (m3rtm). *Proceedings of 2006 IEEE Conference on Radar* (pp. 425–431). doi: 10.1109/RADAR.2006.1631835

Weir, B., & Sokol, T. (2009, May). Radar coordination and resource management in a distributed sensor network using emergent control. *Proceedings SPIE*, *7350*, 73500I. doi: 10.1117/12.818724

Weir, B., & Sokol, T. (2010, April). Scalable self-organizing resource management for multi-function radars in a sensor network. *Proceedings SPIE*, *7698*, 76980U. doi: 10.1117/12.850913

THIS PAGE INTENTIONALLY LEFT BLANK

Initial Distribution List

1. Defense Technical Information Center
   Ft. Belvoir, Virginia

2. Dudley Knox Library
   Naval Postgraduate School
   Monterey, California